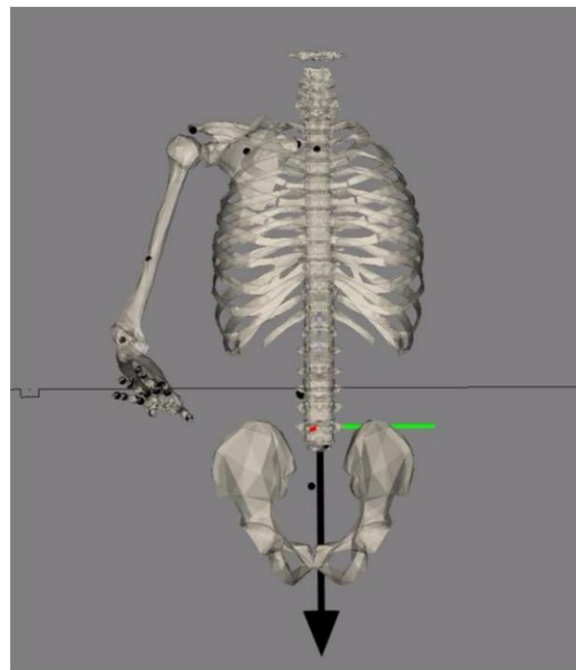


Mathilde de Saint Meloir

Class P2024 – 4th year

# STUDENT-ENGINEER INTERNSHIP REPORT

## Optimization of the pianistic gesture of pressed and struck keys by digital simulation



*Figure 1: Skeletal Model of a Pianist*

**Location of the internship:** S2M Laboratory, University of Montreal, Laval, CANADA

**Dates of the course:** August 30, 2021 – December 17, 2021

**Department where the internship took place:** School of Kinesiology and Sciences of Physical Activity, Faculty of Medicine

**Name of department manager:** Mickaël Begon

**Internship supervised by :** Felipe Verdugo



# Thanks

First of all, I would like to thank Mickaël Begon, full professor at EKSAP and at the Institute of Biomedical Engineering, for having accepted me in his laboratory as a guest student researcher during these 4 months of internship.

I then particularly thank Felipe Verdugo, associate professor and head of research related to piano gesture, for welcoming me into his research team. He trusted me, was able to entrust me with key responsibilities in his research on the biomechanics of the piano and was always able to take the time to support me, to teach me, and to correct me rigorously.

Also, I would like to thank the optimal control team, and more specifically the four doctoral students present, Pierre Puchaud, Eve Charbonneau and Amédéo Cégli, for their precious help which concerned both practical and theoretical subjects.

Finally, I thank all the members of the S2M laboratory for their warm welcome they gave me, and for having made me discover, in great detail, both the world of research and Canada in general.

# Summary

## *Optimization of piano playing thanks to the theory of optimal control*

Professional pianists require daily practice in order to achieve a high level of performance in terms of musical expression and virtuosity. Their practice, which involves the continuous repetition of a wide range of precise and complex attacks, in many cases leads to musculoskeletal disorders (MSDs). Various studies have addressed this problem by analyzing the playing strategies of professional pianists at the level of the upper limbs and the trunk, but no study has yet used digital simulation and optimal control. Being a research method in full effusion, optimization by numerical simulation allows the analysis of this problem eliminating the experimental need to collect data on a large sample of participants. This engineering student internship project aims to use optimal control and digital simulation in order to find innovative kinematic strategies that could allow pianists to reduce their exposure to MSD risks. Based on preliminary research carried out at the Simulation and Modeling of Movement Laboratory, this project integrates into the analysis the entire kinematic chain of pianists (from the pelvis to the fingers) and deals with a specific case of playing: pressed touch and struck touch, types of playing commonly discussed in the literature on the prevention of MSDs in pianists.

**Keywords:** Piano, Music, Biomechanics, Musculoskeletal Disorders, Numerical Simulation, Optimal Control, Kinematics and Kinetics of Movement, Bioptim

# Abstract

## *Optimization of piano playing thanks to optimal control*

Professional pianists require daily practice in order to achieve a high level of performance in terms of musical expression and virtuosity. Their practice, which involves the continuous repetition of a wide range of precise and complex attacks, generates in many cases musculoskeletal disorders (MSD). Numerous studies have investigated this problem by analyzing the playing strategies of professional pianists in the upper limbs and trunk, but no study has yet used computer simulation and optimal control. As a research method in full effusion, the optimization by numerical simulation allows the analysis of this problem replacing the experimental need to collect data on a large sample of participants. This engineering student internship project aims to use optimal control and numerical simulation to find innovative kinematic strategies that could allow pianists to reduce their exposure to MSD risks. Based on previous research conducted at the Motion Simulation and Modeling Laboratory, this project integrates the entire kinematic chain of pianists (from the basin to the fingers) into the analysis and deals with a specific case of playing: the pressed touch and the struck touch, types of playing commonly discussed in the literature on the prevention of MSD in pianists.

**Keywords:** Piano, Music, Biomechanics, musculoskeletal disorders, Numerical simulation, Optimal control, Cinematic and kinetics of motion, Bioptim.

CONFIDENTIAL

# Summary

<b>Introduction .....</b>	<b>8</b>
1/ Pianist context and research on the prevention of injuries among pianists.....	8
<b>Presentation of the laboratory .....</b>	<b>9</b>
<b>Research project.....</b>	<b>11</b>
1/ <b>Problem and objective .....</b>	<b>11</b>
2/ <b>Methodology .....</b>	<b>12</b>
2. 1. Optimal control put into practice with Bioptim.....	12
• <b>2. 1. 1. Optimal control .....</b>	<b>12</b>
• <b>2. 1. 2. The Bioptim bookstore .....</b>	<b>15</b>
2. 2. Development of Optimal Control Programs (OCP) for the two types of affected.....	15
• <b>2. 2. 1. Construction of OCPs.....</b>	<b>16</b>
• <b>2. 2. 2. Development of OCPs .....</b>	<b>20</b>
• <b>2. 2. 3. Solving, Viewing, and Saving OCP Solutions .....</b>	<b>25</b>
2. 3. Optimization of controls: minimization of joint torques.....	26
<b>3/ Results .....</b>	<b>28</b>
3. 1. Results of the staccato hurried games obtained.....	28
• <b>3. 1. 1. Benchmark kinematic solution for a staccato hurried game.....</b>	<b>28</b>
• <b>3. 1. 2. Kinematics solution minimizing upper body distal joints for staccato rush playing .....</b>	<b>31</b>
3. 2. Results of staccato hit games obtained.....	32
• <b>3. 2. 1. Benchmark kinematic solution for a staccato hit game .....</b>	<b>32</b>
• <b>3. 2. 2. Kinematics solution minimizing upper body distal joints for staccato slap game.....</b>	<b>35</b>
<b>4/ Discussion .....</b>	<b>37</b>
4. 1. Commentary and discussion on the staccato pressed stops obtained. ....	37
• <b>4. 1. 1. Commentary on the benchmark solution obtained for a staccato hurried playing.....</b>	<b>37</b>
• <b>4. 1. 2. Commentary on the solution minimizing upper body distal joints for staccato hurried playing.....</b>	<b>38</b>
• <b>4. 1. 3. Comparison of the two solutions obtained for a staccato hurried game .....</b>	<b>38</b>
4. 2. Commentary and discussion on the staccato hits obtained .....	39
• <b>4. 2. 1. Commentary on the benchmark solution obtained for a staccato hit game .....</b>	<b>39</b>

<b>4. 2. 2. Commentary on the solution minimizing the distal joints of the upper body for a staccato slap game.....</b>	<b>40</b>
<b>4. 2. 3. Comparison of the two solutions obtained for a staccato tapped game .....</b>	<b>41</b>
<b>Conclusion.....</b>	<b>42</b>
1/ Technical conclusion .....	42
2/ Personal conclusion .....	42
<b>Bibliography .....</b>	<b>43</b>
<b>Appendix A: Libraries and python functions used.....</b>	<b>44</b>
<b>Appendix B: Dimensions of the bones of the 3D skeletal model .....</b>	<b>45</b>
<b>Appendix C: Bones of the Hand.....</b>	<b>47</b>
<b>Appendix D: Initial position of the skeleton .....</b>	<b>47</b>
<b>Appendix E: Special study on the speed profiles of a hitting and pressing game.....</b>	<b>48</b>
<b>Appendix F: Optimal Solution found 1.....</b>	<b>50</b>
<b>Appendix G: Optimal Solution found 2 .....</b>	<b>50</b>
<b>Appendix H: Optimal Solution found 3 .....</b>	<b>51</b>
<b>Appendix I: Optimal Solution found 4 .....</b>	<b>51</b>
<b>Appendix J: Angular Velocities - Squeezed Clearance.....</b>	<b>52</b>
<b>Appendix K: Angular velocities - slap game.....</b>	<b>52</b>

## Lists of tables

<i>Table 1: Details of the 10 degrees of freedom of the pianist's skeletal model.....</i>	<i>17</i>
<i>Table 2: Initial angular positions of the degrees of freedom of the model.....</i>	<i>20</i>

# Lists of figures

Figure 1: Skeletal model of a pianist .....	1
Figure 2: Photograph of the experimental room of S2M .....	10
Figure 3: Illustration of the "single shooting" method, inspired by Cannon Example, M. Kelly.....	13
Figure 4: Illustration of the "Multiple Shooting" principle, Zhengru Ren.....	14
Figure 5: Graphs of the 3 Optimal Control methods studied.....	15
Figure 6: Defining a Segment in the .Biomod file.....	17
Figure 7: Diagram of dimensions of the modeled piano .....	18
Figure 8: Defining a marker in a file .Biomod.....	18
Figure 9: Representation by Bioviz of the skeletal model and the modeled two-key keyboard.....	19
Figure 10: Average speed profile of the finger during its descent into the key .....	21
Figure 11: The 7 speed values retained from the profile of speed found .....	21
Figure 12: Diagram detailing the 4 phases of the python code produced simulating the Staccato Strike of a note (LA) .....	22
Figure 13: Average speed profile (in ms <sup>-1</sup> ) as a function of time (in s) .....	23
Figure 14: Velocity profile of the finger during its descent into the fingerboard for a pressed game .....	23
Figure 15: Diagram detailing the 4 phases of the python code produced simulating One-Note Staccato Pressed Playing (A) .....	24
Figure 16: Model playing a key with optimized hand position.....	24
Figure 17: Calls to the torque minimization function, checks to optimize .....	26
Figure 18: Explanatory diagram of the minimization functions and call to the MINIMIZE_STATE Bioptim function. ....	27
Figure 19: Contact forces (in N) of the 3 axes of the finger at the bottom of the key as a function of time (s).....	29
Figure 20: Joint positions (in rad) of the 10 degrees of freedom of the model as a function of time (s) .....	30
Figure 21: Articular torques (in Nm) of the 10 degrees of freedom of the model as a function of time (s).....	30
Figure 22: Contact forces (in N) of the 3 axes of the finger at the bottom of the key as a function of time (s).....	31
Figure 23: Contact forces (in N) of the 3 axes of the finger at the bottom of the key as a function of time (s).....	33
Figure 24: Articular positions (in rad) of the 10 degrees of freedom of the model as a function of time (s) .....	34
Figure 25: Articular torques (in Nm) of the 10 degrees of freedom of the model as a function of time (s).....	34
Figure 26: Contact forces (in N) of the 3 axes of the finger at the bottom of the key as a function of time (s).....	36

# Glossaries

ACRONYM	DETAILS
<b>S2M</b>	Motion Simulation and Modeling
<b>UDEM</b>	Montreal university
<b>EKSAP</b>	School of Kinesiology and Sciences of Physical Activity
<b>TMS</b>	Musculoskeletal problems
<b>BIOPTIM</b>	Optimized biomechanics
<b>BIORBD</b>	Biomechanics Rigid Body Dynamics
<b>BIOVIZ</b>	Biomechanical visualization
<b>DDL</b>	Degree of freedom

# Nomenclature

VARIABLE	MEANING	UNITS
<b>X</b>	<b>Differential state variable</b>	-
<b>Q</b>	Position of one joint degree of freedom	[rad]
<b>QDOT</b>	Velocity of a joint degree of freedom (time derivative of Q)	[rad*s-1]
<b>U</b>	<b>Control variable</b>	-
<b>TAU</b>	Actuator / motor torque	[Nm]

# Introduction

This "student engineer" internship took place in Canada at the University of Montreal from August 29, 2022 to December 16, 2022. The project carried out concerns the study of the piano gesture, via digital simulation and the theory of optimal control. The objective is to discover new playing strategies to reduce exposure to risk factors for musculoskeletal disorders (MSDs) related to instrumental practice in professional pianists, by optimizing their movement numerically within the framework of two types of touch. : the pressed touch, and the struck touch.

## 1/ Pianist context and research on the prevention of injuries in pianists

Piano playing represents one of the most complex sensory-motor tasks that humans can perform, requiring years of learning and practice (Furuya and Altenmüller 2013). The enduring and repetitive nature of professional instrumental practice engenders in more than half of professional pianists MSDs during their career (Kaur and Singh 2016). The majority of these disorders appear in the muscles and tendons associated with the distal joints, *ie wrists and fingers* (Bragge, Bialocerkowski, and McMeeken 2006). To minimize exposure to MSD risk factors, pianists could take advantage of multi-joint movement of the upper limbs to better share the load between the distal and proximal muscles (Furuya and Altenmüller 2013). The use of the pelvis and thorax specifically is an adaptable execution strategy that would seem suitable (Verdugo et al. 2020). Beyond the biomechanical constraints, pianists remind us that the interaction between finger and key, generally called "touch", requires requirements of pianistic expression and precision. The study of two types of piano touch predominates scientific research: the struck touch, and the pressed touch. During a "hit" game, the finger begins with a momentum phase where it is at a certain distance from the key. This momentum allows him to arrive already with a certain vertical speed to play the note.

During a "rushed" game, however, this momentum phase is not present. The finger begins the attack by already being in contact with the key, the vertical speed of the finger being zero before the start of the descent of the key. After comparing these two types of hits, Kinoshita et al. (Kinoshita et al. 2007) concluded that, from a biomechanical point of view, the struck touch is a more effective striking strategy, since it allows, among other things, to create a greater vertical velocity of the piano key (especially during producing loud sounds). However, from an acoustic and sound control point of view, Goebel, Bresin, and Galembo 2005 describe pressed touch as the most effective for sound control because it allows better control of the fingerboard mechanism while along the descent of the finger in the key. On the other hand, pressed touch can also contribute to improving the temporal precision between consecutive piano sounds (Goebel and Palmer 2008). Each of these two touches, having their own advantages, are useful for piano playing, which brings together in its repertoire a wide variety of musical contexts. It is thus in this sense that in one of the studies carried out in the S2M laboratory (Verdugo et al. 2020), it is demonstrated that the movement of the trunk can



contribute to the realization of a pressed and struck touch. This study used an experimental research approach, analyzing the movements of 12 expert pianists. At present, the study of this student engineer internship consists of the deepening of this same problem but by a numerical research approach, based on optimal control, using a python library called Biotrim developed in this same laboratory. This numerical approach allows a more detailed analysis of the kinetics of movement, and offers a definite time saving by eliminating the experimental need to collect data on a large sample of participants.

## Presentation of the laboratory

The internship was carried out in Canada at the Laboratory of Simulation and Modeling of Movement (S2M), attached to the School of Kinesiology and Sciences of Physical Activity (EKSAP, Faculty of Medicine) of the University of Montreal on the campus of Laval. This university is the most important in the French-speaking world in terms of research. The S2M laboratory was founded in 2008 by Mickaël Begon (full professor at EKSAP and the Institute of Biomedical Engineering), and brings together three other professors: Felipe Verdugo, associate professor and head of research related to piano gesture, as well as Drs.

Philippe Dixon and Fabien Dal Maso, assistant professors at EKSAP. Each professor has under the supervision of post-doctorates, doctoral students, master's students, and trainees, all specialized in kinesiology, biomedical mechanical engineering, physics or computer science, forming several groups of research projects based on study subjects as well as fundamental (such as the estimation of muscular forces) than applied (for example the design of orthoses).

Each professor develops and supervises a specific research theme in this laboratory: • Team in optimal control – Mickael Begon • Team in neuro-electrophysiology of movement – Fabien Dalmaso • Team in biomechanics and musical performance – Felipe Verdugo • Team in biomechanics and artificial intelligence – Philippe C. Dixon

The common point of the projects found in these four themes is the study of human movement. Some are intended to facilitate injury prevention, while others are intended to improve performance itself. The research topics are very varied. Some projects are, for example, specialized in sports practices, such as the study of the optimization of acrobatics among professional trampolinists, and others in the adaptation of rehabilitation orthoses for adults to the needs of children. These projects, a large part of which focuses specifically on the shoulder and its associated problems, and using state-of-the-art techniques, provide this laboratory with internationally renowned expertise. The laboratory offers state-of-the-art infrastructure for the analysis of human movement: kinetic ergometers, a system of inertial units, 18 Vicon cameras (*optoelectronic* cameras for recording movement), force platforms, various signal capture systems electromyography (EMG), a *Bossendorfer* CEUS grand piano equipped with sensors to record the kinematics of the keys and hammers (

Figure 2), as well as various sports equipment (instrumented treadmill, exercise bike, among others).



*Figure 2: Photograph of the S2M experimental room*

*OpenSpace* work rooms equipped with high-performance computers are also available, organized by technical specialization (optimal control, data analysis, etc.)

# Research project

## **1/ Problem and objective**

Since September 2021, Felipe Verdugo has started a new line of research to study piano gesture through digital simulation and optimal control theory. Biotim, a Python library under constant development in the laboratory thanks to the work of the optimal control team, is an innovative optimization tool for performing numerical simulations based on the theory of optimal control. Optimal control aims to find the optimal motion of a dynamical system by controlling parameters. Grégoire Deshairs, a former trainee in this optimal control team, began in 2021 the development of a pianist skeleton on Biotim playing a succession of notes. The project of this internship will consist in continuing and further developing this dynamic model, while responding to the following objectives and issues.

### ***Plan of the study project***

The objective of the project is to obtain, through the optimal control of knowledge, an insight into new pianistic kinematic strategies allowing to better take advantage of a multi-articular movement of the upper limbs in order to better share the load. between distal and proximal muscles. This objective will be achieved by simulating simple piano tasks taking as optimized controls of the model the joint torques of the joints. The project of this internship will answer the following problem: In order to reduce the occurrence of TMS at the level of the distal limbs in professional pianists, which pianistic kinematic strategies

can be numerically found thanks to the optimal control, for the simulation of simple tasks at the piano ?

The presentation of the study project will be divided into three sections. First, the Biotim library and the optimal control will be presented, then a detailed explanation of the dynamic models based on the optimal control of the two types of touches developed, struck and pressed, will be carried out. Second, the optimal kinematics found for the two different hits will be presented. Finally, the last section proposes a discussion around the presented results.

## 2/ Methodology

### 2. 1. Optimal control put into practice with Bioptim

#### 2. 1. 1. Optimal control

Optimal control (or optimal control) is a branch of mathematical optimization that can be found in many fields such as mechanics, electricity, chemistry, economics, and thus also in biomechanics. This theory applies to all kinds of dynamic systems, such as differential, discrete systems, or systems with noise. An optimal control problem consists in finding a control law which makes it possible to minimize or maximize one or more cost functions such that the controls and the states are optimized, while respecting the imposed constraints. More specifically, an optimal control problem is a set of evolutionary equations.

Each problem (Figure 3) has two state functions  $x(t_f)$  and  $x(t)$ , and a control function  $u(t)$ , which depend on time  $t$ , and which are the parameters of the differential equation of the system of the problem (2). The objective of a problem is to be able to find a control function  $u(t)$  such that the unique trajectory starting from the point 0, associated with this control  $u(t)$ , respects the constraints imposed such as arriving in a time  $T$  at the point 1 with imposed bounds, while minimizing a certain criterion, called the cost.

This sum to be minimized (1) is made up of the Mayer term  $\phi(x(t_f), u(t_f), t_f)$ , expressing an objective that we wish to reach the final moment, as well as the Lagrange term  $\int_0^T Q(x(t), u(t), t) dt$  corresponding to an objective on the whole movement. It is measured at each instant via the integral between 0 and  $T$ .

$$J = \phi(x(t_f), u(t_f), t_f) + \int_0^T Q(x(t), u(t), t) dt \quad (1)$$

Such as, 
$$x(0) = x_0, \quad x(T) = x_1 \quad (2)$$

$$u(0) = u_0$$

$$u(T) = u_1$$

$$\dot{x}(0) = \dot{x}_0$$

$$\dot{x}(T) = \dot{x}_1$$

#### 2. 1. 1. 1. **Single Shooting Method** The so-

called "single shooting" method is the simplest way to transcribe an optimal control problem, and the example of firing a cannon is adequate to represent its operation (Figure 3).

Paramètres :

Fonctions d'état :  $x(t) = \begin{pmatrix} q(t) \\ \dot{q}(t) \end{pmatrix}$

Fonction de contrôle :  $u(t) = F(t)$

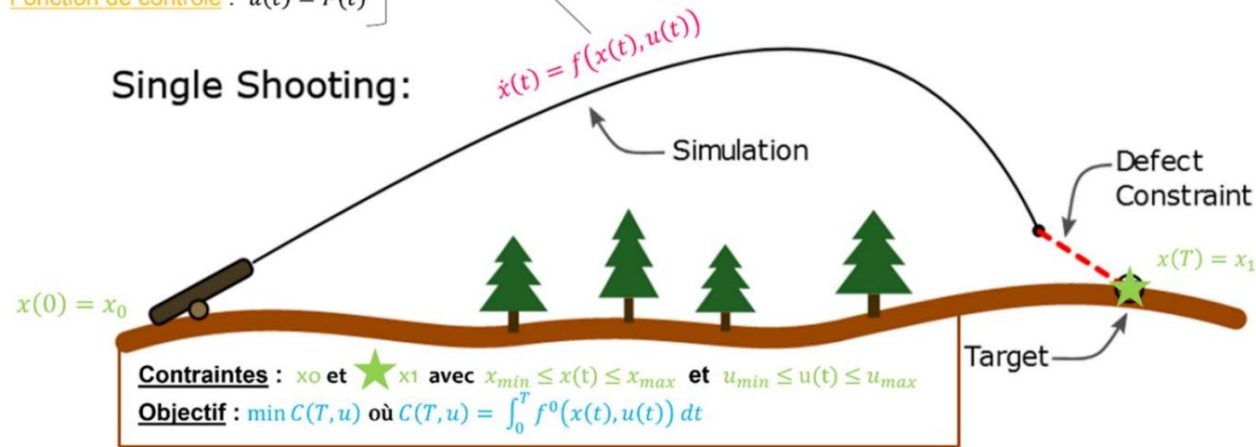


Figure 3: Illustration of the "single shooting" method, inspired by Cannon Example, M. Kelly

The objective of this problem (Figure 3) is to be able to find a firing angle and a quantity of explosive powder, with an initial velocity of the projectile  $\dot{x}(0)$  proportional to this quantity of powder, to put in the barrel. The unique trajectory  $\dot{x}(t)$  of the bullet starting from the cannon  $x(0)$ , taking this angle of fire, must arrive at the target in a time  $T(x(T))$ , while respecting the limit positions  $x_{min}/x_{max}$  and the quantity of powder  $u_{min}/u_{max}$ , and while minimizing the quantity of powder to be used ( $\min C(T, u)$ ).

The "single shooting" method is comparable to what a person could accomplish through a series of experiments: the first shot is made with random values for the state and control variables, then if the target has not been reached (if there is a "defect constraint", see Figure 3) the mass of powder used must be increased. By repeating this method, the target will be reached by minimizing the cost function, i.e. the mass of powder used. From a numerical point of view, each test is a simulation carried out at each iteration by the optimizer.

### 2. 1. 1. 2. Multiple shooting method

When dealing with more complex problems, the "multiple shooting" method will be more suitable. For the direct multiple shooting method, as shown in the figure below (figure 4), the controls ( $u$ ) are discretized and the states ( $x$ ) are evaluated over each integration interval. Each starting point of the integration intervals is called a "shooting node". These starting points correspond to the first integration interval. In this sense, the final node of the interval merges with the starting node of the following integration interval. In the case of a multiple shooting live problem (Figure 4), the integral of the Lagrange function, which was in single shooting the integral between  $t_0$  and  $t_f$ , is thus replaced by a sum over each of the intervals of integration.

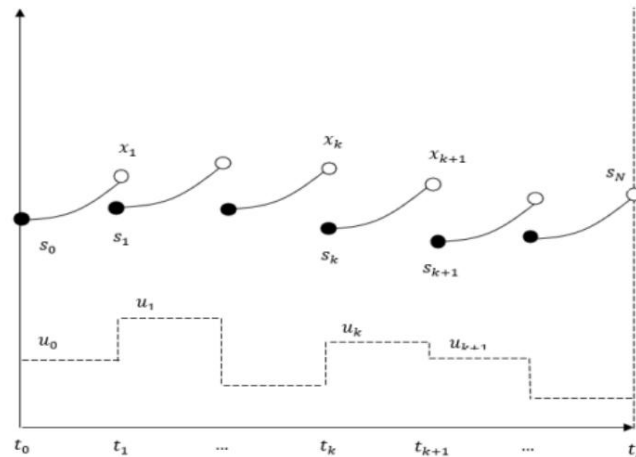


Figure 4: Illustration of the "Multiple Shooting" principle, Zhengru Ren

The simulation time  $\ddot{y} 0$  is divided into  $N$  sub intervals. The values taken at each interval by the  $k$  controls are determined by the solver; in this project, the ma57 linear solver will be used.

$S_0$  corresponds to the starting shooting node,  $S_N$  corresponds to the ending shooting node. At iteration 0, the values of the states at each shooting node are part of the problem definition and constitute the initial solution. As the optimizer begins to find new values at subsequent iterations, the initial integration condition is modified for each interval.

When a simulation is carried out in "direct multiple shooting", a continuity constraint is added. This makes it possible to obtain an evolution of the states which is continuous over time. In other words, for any integer  $i$  in the interval  $[1, N-1]$ , the optimal solution returned must respect the constraint

$$= .$$

### 2. 1. 1. 3. Direct collocation method

Finally, a third type of optimal control program exists, called "direct collocation".

This method is suitable for even more complex problems, where complicated controls and/or path constraints are involved. The principle of this method is close to "direct multiple shooting". However, this method is based on function approximation. The interval between each node is separated by a number of intermediate nodes (polynomial degree) which are found by solving this equation:  $\dot{x} - f(x, u) = 0$ . Best corresponds to the complexity of the phenomenon studied,  $c$  It is this method that is used in this project.

### 2. 1. 1. 4. Summary of the 3 different optimal control methods studied

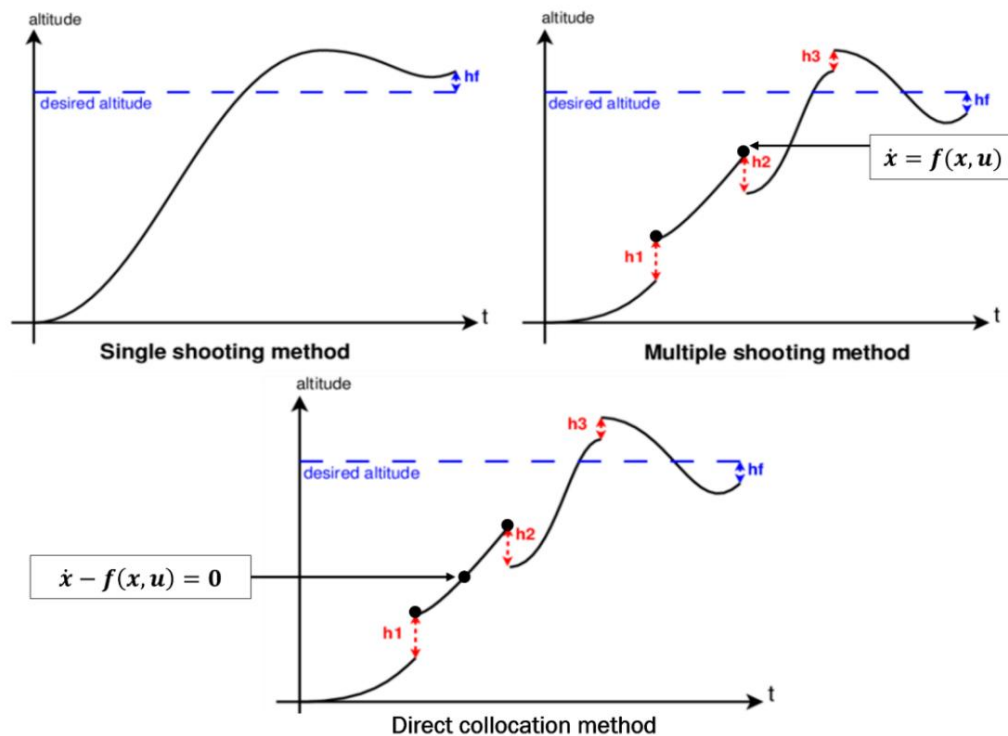


Figure 5: Graphs of the 3 Optimal Control methods studied

### 2. 1. 2. The Biotim library

The library used for this research is called Biotim (for Biomechanical Optimal Control). Biotim is an open-source optimal control Python library suitable for biomechanical study, which mathematically benefits from the powerful algorithmic differentiator provided by CasADi, and which uses the robust and fast optimization problem solvers from Ipopt and Acados. It is composed of sub-libraries: BIORBD (Biomechanics Rigid Body Dynamics), to create musculoskeletal models and manage their direct dynamics.

BIOVIZ (Biomechanics visualization), to visualize these models created on BIORBD.

This bookstore was created by a team from the S2M laboratory, which explains part of their fame. Biotim is thus the basis of the majority of S2M studies relating to the simulation of movement.

## 2. 2. Development of optimal control programs (OCP) of the two types of hits

This project focuses on the search for a kinematic strategy aimed at playing an isolated note according to a pressed touch and a struck touch, while maximizing the use of the proximal limbs in order to limit exposure to MSD risk factors at the distal joints. of the upper limb. This problem thus imposes the creation of two optimal control programs (one for a hit game, and one for a hurry game). In both types of touch, the note is played staccato ( ie.

very fast release of the note after playing), as this type of note duration is commonly used in studies comparing pressed and struck fingerboards.

These two optimal control programs are driven by the joint torques, which means that the controls to be minimized in these two simulations are the joint torques. In order to best estimate how the trunk and the shoulder can contribute to reducing the load on the distal joints, two simulations will be developed by touch. One simulation will minimize the controls at all degrees of freedom of the model equally, and another will further minimize the controls at the degrees of freedom of the finger, wrist, and elbow.

## 2. 2. 1. Construction of OCPs

Before writing these two programs, the import of the libraries grouping together the functions necessary for their operation is done (cf. Appendix A). The main imported Python library is Biopotim, an optimal control library. The usefulness of each of the libraries used will be described later in the report.

First of all, the first stage of this program consists in the development of a skeletal model and a piano keyboard, in order to be able to represent a pianist playing a piano note, the A, of the main octave. . This model is then loaded at the beginning of the program, as many times as there are phases (the number of phases will be developed later).

### 2. 2. 1. 1. Developed piano model

The developed model is a generic rigid-body skeleton. The intern who worked in 2021 on this project started the first development of the model, which was developed and completed during the present internship. This model has a global XYZ axis (respectively red, green and blue) called *ground*, a gravity vector *gravity*  $[0\ 0\ -9.81]$ , a 3-dimensional skeletal model, as well as useful landmarks (markers and contact points) afterwards for the simulation of the model. New parts of the skeleton and their respective degrees of freedom (DOF) were added during this internship (pelvis [1 DOF], thorax [2 DOF], wrist [1 DOF] and finger [1 DOF]). Also, a simplified piano keyboard modeled in 2 dimensions representing two notes (two A at the octave) is modeled. The actual dimensions of a classical piano note and the correct distance from the pianist model to the piano are used. The model is considered isolated from the rest of its environment, there is no interaction with any other solid body that would generate external forces that would apply to the system. Finally, the entire simulation model is stored in a file in *.bioMod format*, and is called in the global code under the name of *biordb\_model*.

• The skeletal model represents an anatomical upper body and right arm. The 3D data of this model, stored in files in *.vtp* format, comes from two *Open Source* skeletal models with similar dimensions: the "Stanford Model" for the wrist and the hand, and the "Wu Model" for the others parts of the skeleton. The dimensions of the bones used are presented in the appendix to this report (see Appendix B). The model has about fifty segments in total, each segment representing a bone or a whole part of the skeleton. They are defined as shown in Figure 6:



```

segment humerus_right ← Nom du segment
parent scapula_right ← Nom du segment parent auquel le segment dépend
RT 0 0 0 xyz -0.00955 -0.034 0.009 ← Matrice de roto-translation et coordonnées de l'origine du
rotations xyz ← Matrice de roto-translation et coordonnées de l'origine du
Degrés de liberté (rotations ou translations)

ranges ← Limites min et max respectives des degrés de liberté.
-pi/2 0.1
-pi/2 pi/2
-pi/4 pi

mass 2.0325 ← Masse en kg du segment
com 0 -0.164502 0 ← Coordonnées du centre de masse
inertia ← Matrice d'inertie du segment
0.011946 0 0
0 0.004121 0
0 0 0.013409

meshfile mesh_files/humerus.vtp ← Fichier .vpt stockant le maillage 3D visuel du segment
endsegment

```

Figure 6: Defining a Segment in the .Biomod file

In order to give a dynamic to this rigid body skeletal model, DOF in x, y or z have been given to the segments involved in a joint. Analogously to reality for a skeletal upper body, the model thus has 10 degrees of freedom (Table 1: Details of the 10 degrees of freedom of the skeletal model pianist).

Table 1: Details of the 10 degrees of freedom of the pianist skeletal model

NAME OF SEGMENT DEGREE OF FREEDOM		- (RADIAN)		+ (RADIAN)	
BOWL	Rot Z	anteversion	$-\ddot{y}/8$	$\ddot{y}/8$	retroversion
THORAX	Rot Y	right rotation	-0.1	0.1	left
	Rot Z	extension	-0.1	0.1	flexion
HUMERUS	Burp X	abduction	$-\ddot{y}/2$		adduction
	Rot Y	external rotation	$-\ddot{y}/2$	$0.1\ddot{y}/2$	Internal
	Rot Z	extension	$-\ddot{y}/4$	$\ddot{y}$	bending
ULNA	Rot Z	extension	$0.053\ddot{y}/4$	-1.48	bending
RADIUS	Rot Y	external rotation	1.48		internal
WRIST	Burp X	extension	$-\ddot{y}/5$	$\ddot{y}/4$	bending
FINGER (INDEX)	Burp x	extension	$-\ddot{y}/4$	$\ddot{y}/4$	bending

ÿ The simplified piano keyboard model is in 2 dimensions and represents the longitudinal section of a piano keyboard with only the presence of a key actually used. During the development process, two notes were modeled, but only one is used to respond to the piano task chosen for the simulation. The two keys are modeled by 1 slotted segment, and the keyboard by an alignment of 3 lines. By taking as a reference measurements collected during preliminary studies at the S2M laboratory on the

pianists, the middle of the top of the lowest key of the keyboard is located at 55.5 cm in x, -16.1 cm in y and 6.8 cm in z in the center of the pianist's thorax. Here are the measurements of the piano keyboard model:

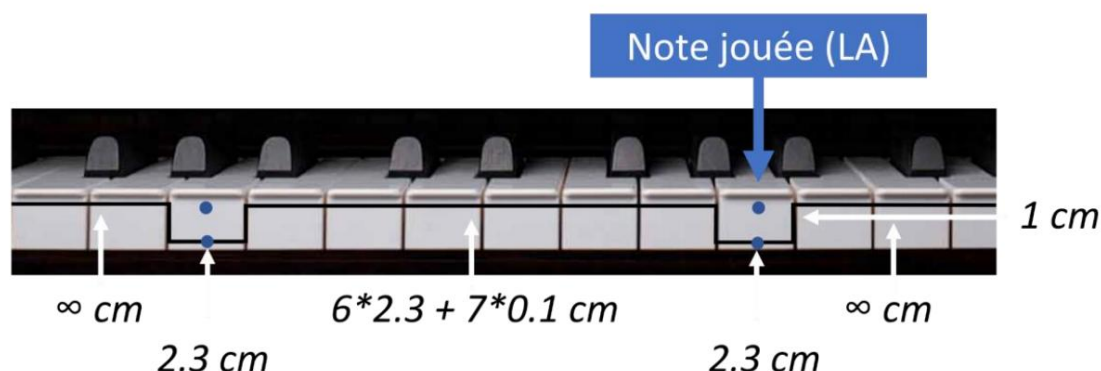


Figure 7: Diagram of the dimensions of the modeled piano

ÿ The global model also integrates different markers used for the simulation of the skeletal model. They are necessary to constrain the model to perform a certain piano playing in space, by imposing on the index finger to superimpose its marker on the two markers of the key played in order to simulate the playing of this note. Two markers are therefore placed above and below the center of the 1st and 2nd key, and one marker is placed at the end of each finger of the hand. These markers have a name, a parent and an xyz position relative to their parent's landmark (Figure 8).

marker finger_marker	←	Nom du marker
parent 2distph	←	Nom de son parent
position 0.0025 -0.015 0.0005	←	Position par rapport à son parent
endmarker	←	Clôture du marker

Figure 8: Defining a marker in a .Biomod file

ÿ Finally, the model has a contact point placed at the end of the finger playing the keys, which is also used for the simulation of the skeletal model. This contact point has the same characteristics as the markers but with its dimension, according to the 3 axes xy and z.

Figure 9 shows a complete representation of the developed pianist and piano, displayed thanks to the Bioptim library called "Bioviz", where the global axis, all the local axes, the gravity vector (black arrow pointing down), as well that the markers and contact points are represented. The wrist and the hand bring together a large number of degrees of freedom, which is why the representation of their respective axes below is very difficult to read in this area.

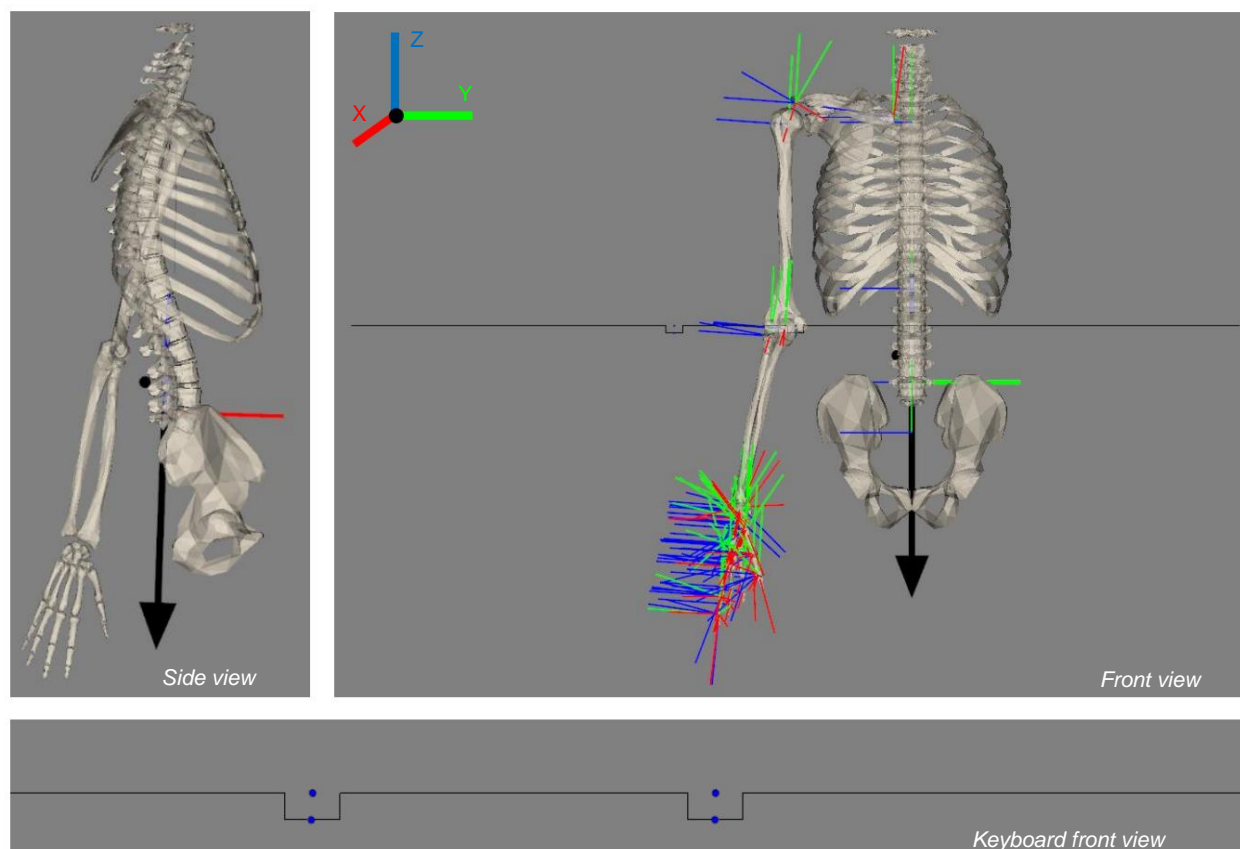


Figure 9: Representation by Bioviz of the skeletal model and the modeled two-key keyboard

### 2. 2. 1. 2. Dynamics and limits of the states and controls of the two programs

As explained previously, the dynamics of the model are controlled by generalized forces. These generalized forces are forces and moments directly applied to each degree of freedom of the model, as if virtual motors were to feed them. In Bioprim, this dynamic is called "torque driven", or *Torque\_Driven*. In torque-driven dynamics, the states are the positions (also called generalized coordinates,  $q$ ) and the velocities (also called generalized velocities,  $\dot{q}$ ) and the commands, or controls, are the joint torques (also called generalized tau forces).

Finally, before talking about the spatio-temporal functions of each phase of the simulation, it is important to first define the boundary and initial conditions of the positions ( $q$ ) and the velocities ( $\dot{q}$ ), as well as the controls ( $\tau$ ), consistent with the joint degree of freedom limits already defined in the *bioMod* file. However, in order to simplify the simulation, the initial state of the model is positioned at the location where the skeleton with the index finger rests on the key. The joint positions of each DOF in this position were thus recorded (Table 2), and given in the initial position (cf. Appendix D). Also, the limits of the DOF of the pelvis and the thorax were imposed null for the 1st point and the last moment of the simulation so that the model begins and ends with a "neutral" posture at the level of the trunk, such as the pianists would aim in context of practice or performance. Except for these positions

initial and final, the other boundary conditions are applied to the first point, to all the intermediate points, as well as to the last point.

Table 2: Initial angular positions of the degrees of freedom of the model

SEGMENT	Basin	Thorax			Humerus			Ulna Radius Wrist Index		
DDL	Rot Z	Rot Y	Rot Z		Burp X	Rot Y	Rot Z	Rot Z	Rot Y	
Angle (rad)	0	0	0		0	0.08	0.67	1.11	1.48	0
										0.17

## 2. 2. 2. Development of OCPs

A complex dynamic movement to be optimized must be sequenced in different phases. Thus, at each stage of the attack, a new phase must be defined: finger run-up outside the key, play inside the key, voluntary pause time before a hurried play, etc. Each of the phases must be defined by a time and a number of nodes (or shooting nodes), initial states and controls and limits, and may have its own objectives, dynamics, constraints, functions dedicated to the transition with the next phase, and multiple other functions.

### 2. 2. 2. 1. Staccato Frappé Game – Definitions and specific functions of each phase

[The first phase of a slap game \(phase 0\)](#) (Figure 12) Figure 12: Diagram detailing the 4 phases of the python code produced simulating the Staccato Frappé Game of a note (LA)) consists for the index to gain momentum in order to start playing the key with a certain non-zero speed. The only constraint imposed on the index finger is to start and end this phase with its fingertip marker superimposed on the marker positioned in the center of the key played (constraint called SUPERIMPOSE\_MARKERS on Bioprim). Otherwise, the hand can take the trajectory that it wishes throughout the phase in order to anticipate in the most optimal manner possible the next phase of depression of the key. In order to give the model time for this take-off, a time of 0.3 seconds, segmented into 30 shooting knots, was imposed for this phase.

[The second phase of hit play \(phase 1\)](#) (Figure 12) represents the descent of the finger inside the key. In order to ensure a beautiful sound at the exit of this attack of LA struck in staccato, the pianists control their descent into the key with a very particular velocity profile. A particular study (cf. Appendix E) thus had to be carried out in order to find the data of this velocity profile plotted in Figure 10 and imposed on the finger throughout its descent into the key. It is with the experimental data collected and analyzed beforehand at the S2M laboratory that this particular study was carried out.

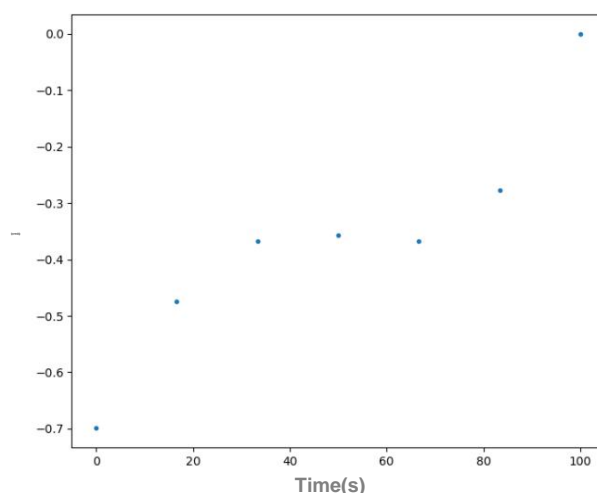


Figure 10: Average velocity profile of the finger as it descends into the key

During the second phase of this struck game, the index finger is thus constrained during its descent phase in the key to the velocity profile obtained above (constraint called TRACK\_MARKERS\_VELOCITY on Biotim). Still thanks to this particular study, 6 shooting nodes were imposed on this phase (by comparing the number of frames, found thanks to these same experimental data, to the theoretical number of shooting nodes of a phase) and a duration of 0.027 seconds (according to the equality of 150 frames = 1 sec). 7 values of this speed curve are thus retained (Figure 11): 6 values for the 6 shooting knots of the phase, and 1 last value for the first knot of the following phase.

```
vel_push_array2 = [[-0.698417100906372, -0.474601301515033, -0.368024758139809, -0.357349785081633,
                    -0.367995643393795, -0.277969583506421, 0]]
```

Figure 11: The 7 speed values retained from the speed profile found

Also, in order to order the finger to finish the phase at the bottom of the modeled key, the index finger is again forced to superimpose its marker on the marker at the bottom of the key at the end of this phase.

During the transition between the second and the third phase of this struck game, i.e. at the moment when the index finger touches the bottom of the key, an impact is imposed (IMPACT function on Biotim) which theoretically allows a discontinuity of the speeds at a moment T, and which thus generates an acceleration which tends towards infinity for an infinitely small instant. Physically, this impact allows an infinitely small contact time when the index finger reaches the bottom of the key.

The third phase of this hit game (phase 2) (Figure 12) represents the moment when the finger remains at the bottom of the key before leaving. According to the particular study cited above, this phase is composed according to the experimental data of 9 frames, and thus of 9 shooting nodes, and lasts on average 0.058 seconds. This imposed contact (constraint called TRACK\_CONTACT\_FORCES on Biotim) consists in following the reaction forces of the x, y and z axes of the touch on the finger, without acceleration point, towards given limit targets. These reaction forces depend on the sound intensity and the type of touch of the playing, in this case being a type of staccato touch on a grand piano. According to Gillespie's article, *The MIT Press* hand. An interval of [0, 30] N is thus constrained for the directed contact in z. , 2011 [3], a fortissimo game can generate forces in z of up to 30 N on Minor forces being

also generated in x and in y on the finger, an arbitrary limit interval of  $[-5, 5]$  N was imposed for these two contacts.

Finally, the fourth and last phase of this batting game (phase 3) (Figure 12) represents the moment of the attack when the index finger releases the key. Arbitrarily, a time of 0.3 seconds with 30 knots of shooting was defined for the realization of this phase in order to give time to the model to find, with the trajectory that it wishes, a final position of attack. The only constraints imposed on the model for this final position are firstly that the index marker ends up superimposed on the top marker of the key as for the initial position, and secondly that the articular angles of the pelvis and the thorax end up null.

The game of an LA struck staccato produced by the skeletal model is thus composed of the 4 phases defined previously, each composed of a time and a number of calculated or arbitrary shooting nodes, and structured by constraints and objectives which are clean. All these data specific to a FRAPPE game are thus gathered in Figure 12 below. A frontal view of the key modeled and played is present, and is displayed the position of the tip of the index finger playing the key at each of the phases. The distance between the marker at the top of the played key and the origin of the marker is also specified there.

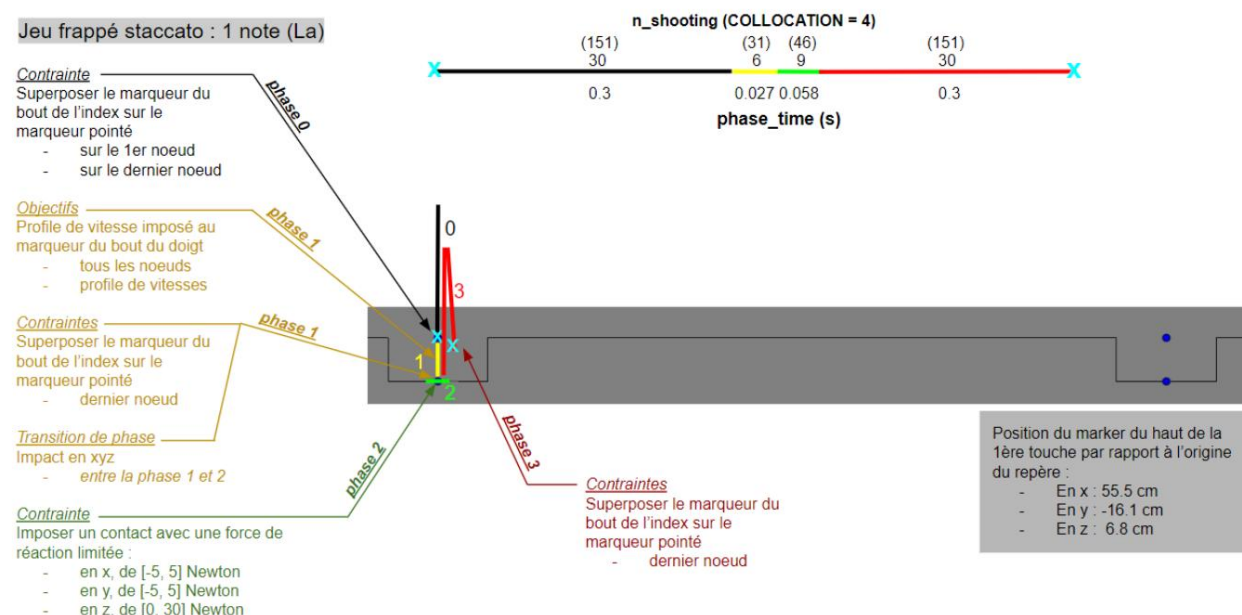


Figure 12: Diagram detailing the 4 phases of the python code created simulating the One-Note Staccato Strike Game (LA)

## 2. 2. 2. 2. Staccato Squeeze Play – Definitions and Specific Functions of Each Phase

Staccato squeeze play is very similar to staccato slap play. Only the differences distinguishing the modeled pressed game from the struck game are therefore presented in this part.

### Phase 0 (Figure 15) \_

While during the first phase of the attack of the touch the batting game gives the hand an arbitrary amount of time to gain momentum, the rush game begins with a static phase where the player is asked to finger to remain on the key for a few milliseconds, before playing the note. He is

CONFIDENTIAL

imposed on the index finger to leave its marker superimposed on the marker at the top of the key throughout this first stage of the attack.

#### Phase 1 (Figure 15)

The second difference is that playing in a hurry is also characterized by a very specific speed profile during the descent of the finger into the fingerboard, a profile similarly deriving from the specific study carried out (see Appendix E) with the experimental data collected and analyzed beforehand. at the S2M laboratory (Figure 13).

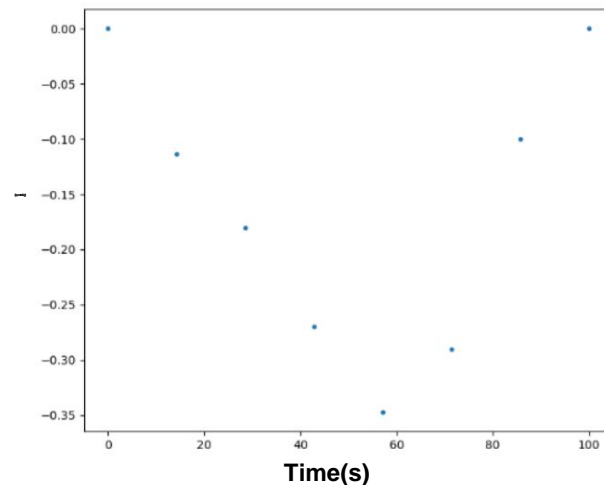


Figure 13: Average velocity profile (in ms<sup>-1</sup>) as a function of time (in s)

Figure 14 presents the 7 values representing this speed profile (for the 7 shooting knots of this phase) thus imposed on the index finger throughout its descent into the key. For a hurried game, the finger how well, as previously defined, by a zero speed value unlike the hit game.

```
vel_push_array2 = [[0, -0.113772161006927, -0.180575996580578, -0.270097219830468,
                    -0.347421549388341, -0.290588704744975, -0.0996376128423782, 0]]
```

Figure 14: Velocity profile of the finger during its descent into the key for a pressed game

#### All phases (Figure 15)

Recently, still thanks to the particular study carried out on experimental data collected by the S2M laboratory, the number of shooting nodes, and the average time of the second and third phase of a hurried game have been defined. The second phase, which represents the descent of the finger into the key, is composed of 7 shooting nodes and lasts 0.044 seconds, and the third phase, which represents the phase of contact of the finger at the bottom of the key, is similarly composed of 7 knots, and lasts 0.051 seconds.

Figure 15 below summarizes the simulated staccato pressed game where all the data specific to this type of attack is exposed: the time (phase\_time) and the number of shooting nodes (n\_shooting) of each phase, their constrained functions and objectives specific, and more.



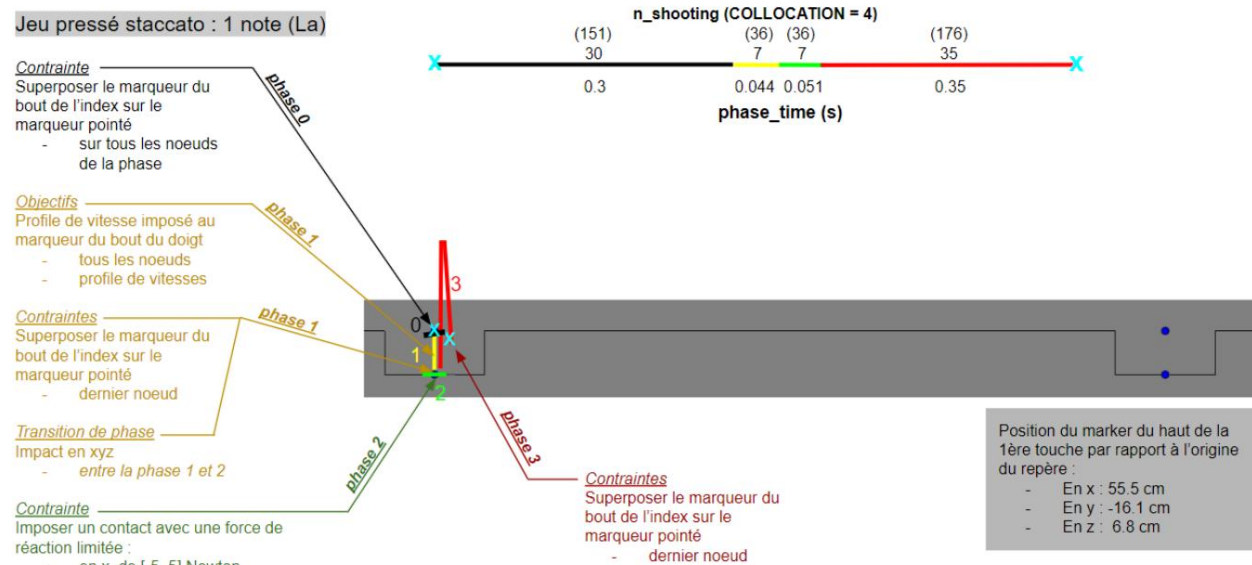


Figure 15: Diagram detailing the 4 phases of the python code produced simulating the Pressed Staccato Play of a note (LA)

### 2. 2. 2. 3. Spatial constraints common to both touches

#### Spatial Constraint - Upturned Hand Gravity makes

it less constraining, and thus more optimal, for the model to play the piano note with the palm of the hand upturned (Figure 16). A constrained function is therefore created to force the model to “straighten” its hand, such as the pianists would position themselves in a practice context. The constraint consists in imposing on the marker placed at the end of the little finger to always be placed to the anatomical right of the marker placed at the end of the index (Name of the constraint in the two Python codes developed (“True\_Pianooptim” [2021] 2022): custom\_func\_track\_finger\_5\_on\_the\_right\_of\_principal\_finger).

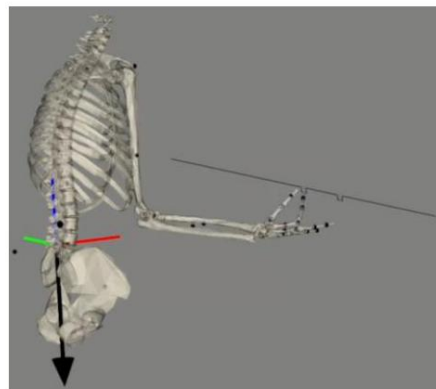


Figure 16: Model playing a key with optimized hand position without imposed straightening function



### **Fixed Spatial Constraint - Key Background.**

When attacking the key, although the model's index finger only has to reach the marker positioned at the bottom of the key before leaving it, part of the hand can still end up cross the note boundaries modeled in 2 dimensions, which would corrupt the real spatial constraints. To prevent the model from crossing the key in this way, a fixed spatial constraint in Z is imposed throughout the attack: the marker of the index and the little finger of the hand cannot go lower than the bottom of the key (Name of the constraint in the two Python codes developed ("True\_Pianoptim" 2021): `custom_func_track_principal_finger_and_finger5_above_bed_key`).

### **Momentum Goal - Keep control in a single plane.**

To prevent the model from playing the attack of the key with his hand tilted, effect of gravity, a dynamic objective is imposed on him allowing him to keep his hand in a single plane throughout the game, as pianists would naturally do. in the context of practice or performance. This objective requires the segment of the index (composed of the proximal, median and distal phalanx of the index, having only one degree of freedom at the origin of the proximal phalanx) and the metacarpus of the index (cf . Appendix C) to remain as perpendicular as possible to the global Y axis, directed in the longitudinal direction of the modeled piano keyboard (Name of the objective in the two Python codes developed ("True\_Pianoptim" 2021): `custom_func_track_principal_finger_pi_in_two_global_axis`).

## **2. 2. 3. Solving, displaying and saving OCP solutions**

The Biotim Python library optimizes the two developed programs, modeling the two different keystrokes, thanks to its Python class called "OptimalControlProgram" (OCP). In order for the optimization to take into account all the programmed elements of the simulation, the key arguments developed in the two programs are sent to this class, i.e. the model, the time of the phases and their number of "nodes". of shooting", the initial conditions and imposed limits, all the constraints and objectives of each phase, and finally the solver used, which is "ode\_solver" in

our case.

### **2. 2. 3. 1. Resolution of OCPs**

In this study, it is the linear solver "ma57" in COLLOCATION, with a polynomial degree of 4 (Figure 5), which is used. When solving programs, a function allows the display of live optimization graphs: graphs of states (angular positions and angular velocities), controls (joint torques) and contact forces. Chart updates are displayed in real time. The values of goals and constraints are also displayed on a live graph, helping for example to know if the goals and constraints are respected, which can later help in debugging the code.

### **2. 2. 3. 2. Display of the results**

First, after the resolution made, all the final graphs thus exposing the optimal solution found of the states, the controls, the contact forces applied on the tip of the index, and the objectives And

constraints, are displayed. The resolution time of the optimal program is also annotated. On the graph displaying the contact forces applied to the tip of the index finger, the values of the contact forces change strangely at each moment of the attack for numerical reasons. The value to be retained for each instant, being the only one which respects the imposed limits, is the first value displayed.

Second, the individual cost of goals, functions, and constraints is also displayed in the program console.

Lastly, the main parameters of the solution obtained (states and controls) are saved as a dictionary in a .pckl file, in order to be able to independently display the animation of the solution found in another independent code.

### **2. 2. 3. 3. Code for displaying the animation of the optimal solution found**

In order to display the animation of the optimal solution found, an autonomous code was developed using the Python library Bioviz. In this code, the file that gathers all the important data saved in .pckl format (states and controls) is retrieved, as well as the .bioMod model file. Display parameters are also specified there, such as the size of markers, contacts and the display of the global marker. And it is thus thanks to all the positions  $q$  recorded that the optimized piano gesture obtained is displayed and animated.

## **2. 3. Optimization of controls: minimization of joint torques**

The objective of this project is to use the theory of optimal control to find an optimized piano kinematic strategy for a single note playing, limiting the use of the distal members of the model. This is why two programs have thus been developed in the previous part tending to represent as realistically as possible two piano key attacks (a hurried game, and a staccato struck game), and controlling the minimization of the articular torques of the distal joints of the model.

Here below (Figure 17) the main objective functions of these two codes which make it possible to minimize, with a more or less significant weight, the joint torques of the 10 joints of this model. In these functions, called MINIMIZE\_CONTROL on Bioprim, it is indeed the "tau" pairs that we minimize. The weight of this arbitrarily chosen objective is 100. This weight represents the prioritization of the minimizations of the joint torques of the model: the larger this weight, the more this minimization function will be prioritized and thus used. The objective of this function is therefore to find the minimum torque of each joint which manages to respect all the constrained functions and objectives of the problem.

```
objective_functions = ObjectiveList()
objective_functions.add(ObjectiveFcn.Lagrange.MINIMIZE_CONTROL, key="tau", phase=0, weight=100)
objective_functions.add(ObjectiveFcn.Lagrange.MINIMIZE_CONTROL, key="tau", phase=1, weight=100)
objective_functions.add(ObjectiveFcn.Lagrange.MINIMIZE_CONTROL, key="tau", phase=2, weight=100)
objective_functions.add(ObjectiveFcn.Lagrange.MINIMIZE_CONTROL, key="tau", phase=3, weight=100)
```

*Figure 17: Calls to the torque minimization function, checks to be optimized*

The search for minimum may not have a unique solution in an optimal control problem with many variables. For example, for the same objective function value, in some cases we can find different values for the problem's decision variables.

In such a case, the optimization is said to be on a local optimum plateau. To have convergence and create more minima on the plateau, we say that we must convexify the cost function (cf. Figure 18). We can then add a regularization term, in this case a minimization for the velocity states (Figure 18). Its weight is much lower than the weight of the main objective of the cost function (here to minimize the pairs) but it suffices to create local minima to obtain convergence if one did not obtain any, or more quickly if one already obtained some. In Figure 18, an illustration of the convexification of the cost function.

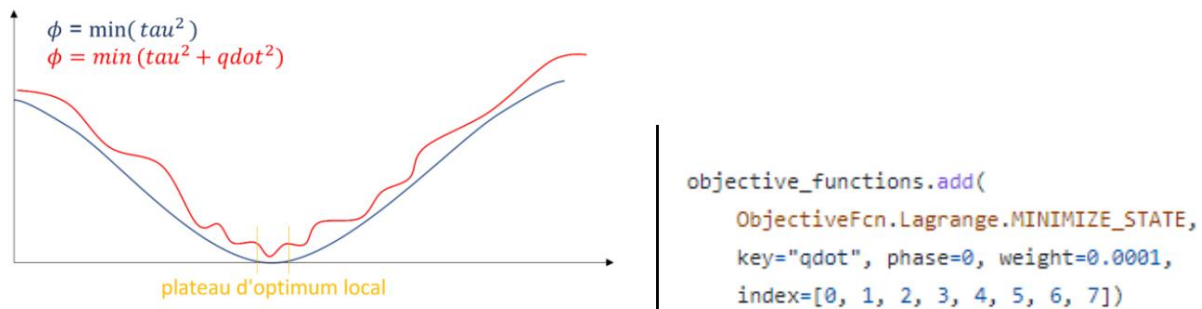


Figure 18: Explanatory diagram of the minimization functions and call of the MINIMIZE\_STATE Bioptim function.

## 3/ Results

In order to find the piano movement that realistically achieves these two types of key attacks and which limits the joint use of the finger, the hand and the elbow (the joints most affected when musculoskeletal disorders appear in pianists.), the two developed programs are launched with specific joint minimizing weight combinations.

✚ First, a benchmark kinematic simulation is launched for both types of touch with a common minimization of joint torques applied by default, presented above, with a weight of 100. All joints are thus prioritized equally, the model is free to choose the most optimal gesture, no articulation is preserved.

✚ Then, this time with the aim of preserving the use of the joint torques that are more likely to witness the appearance of long-term injuries (distal joints), a second specific kinematic simulation is launched in both cases (pressed play and slapped play). The joints of the finger, the index finger, the wrist (at the level of the semilunar area of the wrist (cf. Appendix C)), and the elbow (ulna (extension/flexion) and radius (internal external rotation)) are thus minimized with a weight of 10,000, while the other joints remain minimized only with a weight of 100. As a result, the use of the joints to be preserved, having a minimization function with a greater weight, are thus minimized in priority throughout the movement. Also, the weight of the objective functions forming the dynamics of the movement which are essential for the proper functioning of the desired gesture, is similarly increased so that these objectives remain, despite greater prioritization of certain joints, taken into account. All the weights of these objective dynamic functions are therefore multiplied by a factor of 50 for these two test simulations.

### 3. 1. Results of staccato pressing games obtained

#### 3. 1. 1. Benchmark cinematic solution for staccato rush playing

For the cue kinematic simulation performed for a staccato rush game minimizing the torque of all upper body joints as much, an optimal solution was found. The program took 193 seconds to find this controlled optimal solution (see Appendix F) with 72 iterations. The total sum of the costs of his objectives is  $7.001e+03$  (cost of an objective = weight\*values). The main data of the optimal kinematic solution found as a function of time are displayed in Figure 19, Figure 20 and Figure 21. Each phase of the simulation is delimited by a vertical dotted line.

First of all, Figure 20 below shows in orange the joint position in radians of each of the 10 degrees of freedom of the model. It can be observed that the articular positions of the pelvis (anteversion/retroversion) and of the thorax (right/left rotation and extension/flexion) vary within an interval of  $0.1 \pm 0.05$  rad maximum, and that the articular positions of the humerus in abduction /adduction (rotX) and in external/internal rotation (rotY) vary within an interval of  $0.4 \pm 0.05$  rad. During the last phase, when the finger leaves the key, the position of the ulna joint, starting from an angle of  $1.1 \pm 0.1$  rad, forms a concave curve until the end of the gesture reaching a maximum bending of  $2.15 \pm 0.1$  rad. The wrist joint (lunate) varies by an angle of  $0.7 \pm 0.1$  rad, and  $0.8 \pm 0.1$  respectively

rad during the 1st and last phase. Finally, the finger (2proxph\_2mcp) varies following a convex curve dropping to a minimum of  $0.2 \pm 0.05$  rad during the contact phase of the finger at the bottom of the key. The joint velocities in rad/s of the same degrees of freedom as a function of time are presented in Appendix J.

Still for each of these 10 degrees of freedom, Figure 21 below shows in orange their joint torque in Nm as a function of time (s). The articular torque of the pelvis, in anteversion(-)/retroversion(+), varies within an interval of 0 to -1.2 Nm. Starting from zero torque, the thorax in flexion/extension (rotZ) reached during the first phase of the attacks a torque of  $4 \text{ Nm} \pm 0.2$ , remains within  $0.5 \pm 0.1$  Nm of this value, then drops again during the last phase to zero torque. The joint torques of the wrist, and of the finger, reach a peak only during the contact phase respectively at  $-4.6 \pm 0.1$  and at  $-2.4 \pm 0.1$  Nm.

Figure 19 below represents the contact forces, along the 3 axes, present during the contact between the tip of the index finger and the bottom of the piano key when playing the key. These contact forces vary from  $-5$  to  $5 \pm 0.2$  N in X and Y, and from 0 to  $30 \pm 1$  N in Z.

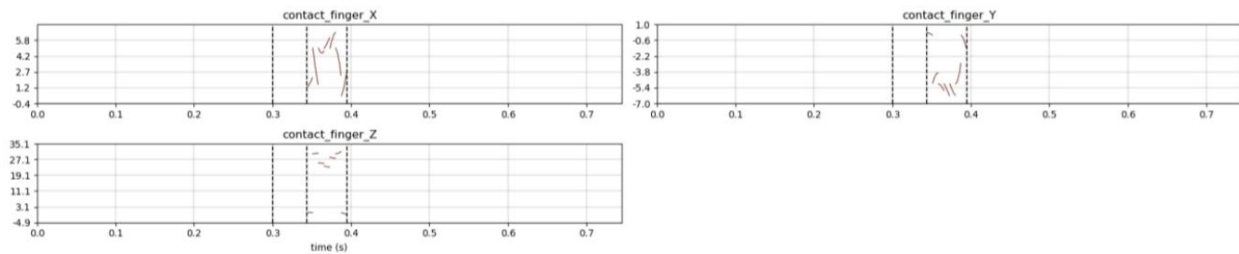


Figure 19: Contact forces (in N) of the 3 axes of the finger at the bottom of the key as a function of time (s).

### Animation of the solution

The optimized solution can be animated thanks to an external code presented previously in the "methodology" part. This animation thus represents the skeletal model of the pianist playing the game of an "A" in staccato pressed attack. It can be viewed at the following links: Front view: <https://drive.google.com/file/d/1CgHDY3k8MtWlU2YIbNA0ksEvSzc9bwlJsE/view>

Side view: [https://drive.google.com/file/d/1kYRK\\_y0H-T0RtUqBR3\\_QZLMVYtJHm0td/view](https://drive.google.com/file/d/1kYRK_y0H-T0RtUqBR3_QZLMVYtJHm0td/view)

### States (q) of limbs by minimizing more the finger, hand, radius & ulna for a staccato pressed attack of one key.

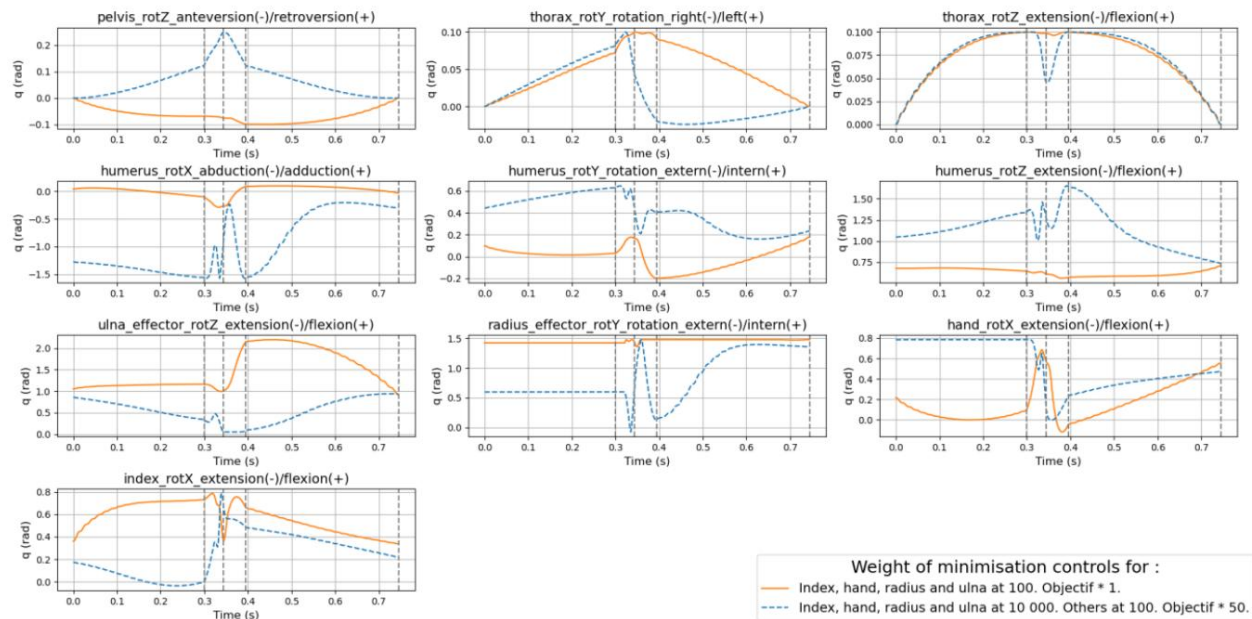


Figure 20: Joint positions (in rad) of the 10 degrees of freedom of the model as a function of time (s) for two different simulations of a hurried game

### Torque (tau) of limbs by minimizing more the finger, hand, radius & ulna for a staccato pressed attack of one key.

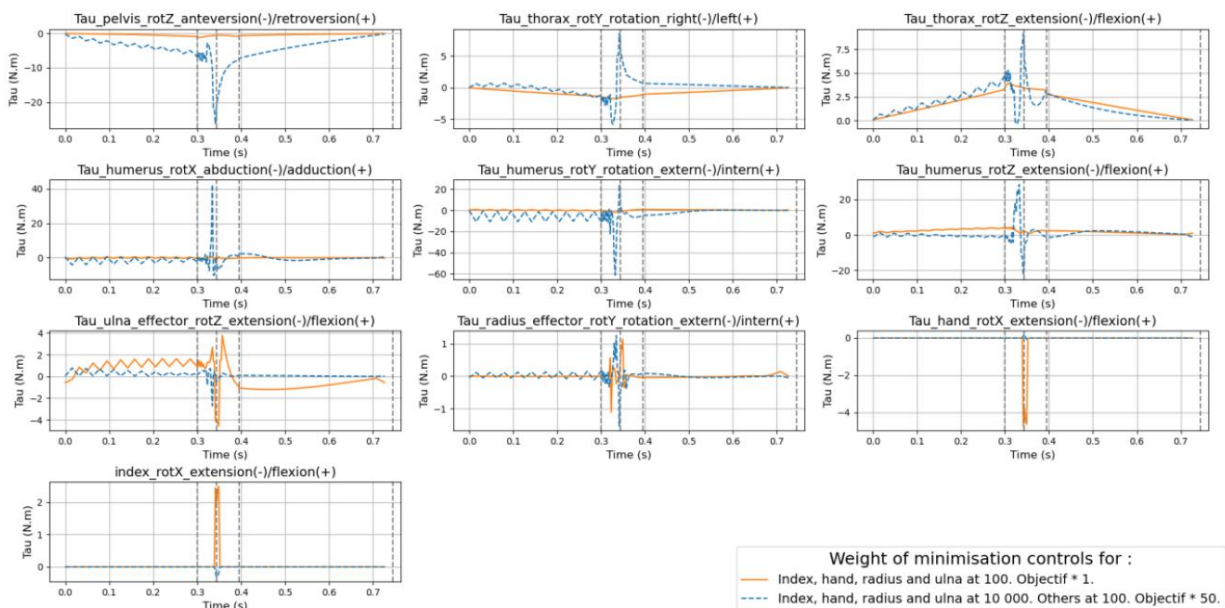


Figure 21: Joint torques (in Nm) of the 10 degrees of freedom of the model as a function of time (s) for two different simulations of pressed play.

### 3. 1. 2. Kinematic solution minimizing upper body distal joints for a game staccato hurry

For the particular kinematic simulation performed for a rushed staccato game minimizing in priority the torque of the distal joints of the upper body, an optimal solution was found. The program took 487.50 seconds to find this controlled optimal solution (see Appendix G) with 179 iterations.

The sum total of his lens costs is  $2.5032e+05$  (lens size = weight\*values). The main data of the optimal kinematic solution found as a function of time are displayed in blue in Figure 20, Figure 21 and Figure 22 above. Each phase of the simulation is delimited by a vertical dotted line.

First, Figure 20 above outlines in blue the joint position in radians of each of the model's 10 degrees of freedom. It is observed that the joints of the pelvis (anteversion/retroversion) and of the thorax (right/left rotation and extension/flexion) vary respectively in an interval ranging from 0 to  $0.25 \pm 0.02$  rad, and from 0 to  $0.1 \pm 0.01$  rad. The articulation of the humerus in abduction/adduction (rotX) reaches an angle of -1.5 rad when the finger has just come into contact with the bottom of the fingerboard, and when the hand resumes the attack. The joint velocities in radians per second of the same degrees of freedom as a function of time are presented in Appendix J.

Still for each of these 10 degrees of freedom, Figure 21 above shows in blue their joint torque is displayed in Newton meters as a function of time in seconds. It can be observed there that when the finger descends inside the fingerboard, the joint torque of the pelvis (anteversion/retroversion) goes from  $-2 \pm 1$  Nm at the first instant of descent, to  $-23.1 \text{ Nm} \pm 2$  Nm at last moment of the descent. The torques of the thorax joint (rotation X, right/left rotation and rotation Z, extension/flexion) pass during this same phase respectively from  $-5 \pm 1$  Nm to  $10 \pm 1$  Nm, and from 0 to  $8 \pm 0.5$  Nm. The torque of the humerus in abduction/adduction (rotX) and in external/internal rotation (rotY) varies within an interval ranging from -10 to  $42.5 \pm 4$  N.m also during the descent phase of the finger in the fingerboard. In external/internal rotation, and in extension/flexion, the torque of the humerus varies respectively between  $-57.5$  and  $20.5 \pm 4$  N.m and between -22 and  $28 \pm 3$  Nm. Finally, the joint torque of the wrist (lunate) varies in an interval of  $0.2 \text{ Nm} \pm 0.05$  in an interval of  $-0.35 \pm 0.05$  Nm, and that during the phase of contact of the finger at the bottom of the

, and the finger couple

hit.

Figure 22 below represents the contact forces, along the 3 axes, present during the contact between the tip of the index finger and the bottom of the piano key when playing the key. These contact forces vary from  $-5$  to  $0 \pm 0.2$  N in X and Y, and stagnate at  $0 \pm 0.1$  N in Z.

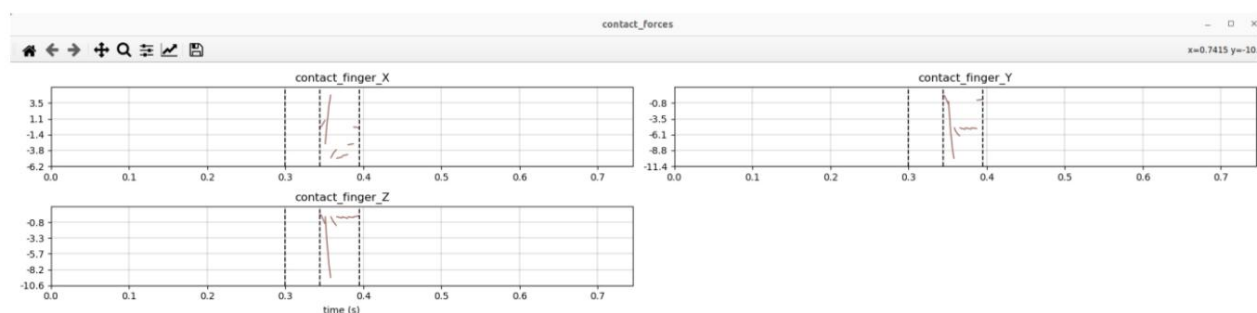


Figure 22: Contact forces (in N) of the 3 axes of the finger at the bottom of the key as a function of time (s).

CONFIDENTIAL



### **Animation of the solution**

The animation of this specific kinematic solution thus represents the skeletal model of a pianist playing the game of an LA in staccato pressed attack, with a minimization imposed on the 4 distal joints of the upper body, in other words the finger, the wrist, radius and ulna.

It can be viewed on the following links: Front view:

[https://drive.google.com/file/d/1PWsM3ZuZzxMIPUbjAyc7GVZIDERli\\_rF/view](https://drive.google.com/file/d/1PWsM3ZuZzxMIPUbjAyc7GVZIDERli_rF/view) Side view: [https://drive.google.com/file/d/1dd1LQaeEjyPIgSHw\\_f93DP0qNIABwSwF/view](https://drive.google.com/file/d/1dd1LQaeEjyPIgSHw_f93DP0qNIABwSwF/view)

## **3. 2. Results of staccato hit games obtained**

### **3. 2. 1. Benchmark kinematic solution for a staccato hit game**

For the cue kinematic simulation performed for a staccato hit game minimizing the torque of all upper body joints as much, an optimal solution was found. The program took 183.98 seconds to find this controlled optimal solution (see Appendix H) with 71 iterations. The total sum of the costs of his objectives is  $1.878e+05$  (size of an objective = weight\*values). The main data of the optimal kinematic solution found as a function of time are displayed in Figure 23, Figure 24 and Figure 25 below. Each phase of the simulation is delimited by a vertical dotted line.

First of all, Figure 24 below shows in orange the joint position in radians of each of the 10 degrees of freedom of the model for this simulation. It can be observed that the pelvic joint reaches an angle of  $-0.1 \pm 0.02$  rad by anteversion just before the finger presses the key, before returning to a zero angle from the end of the contact phase at the bottom of the key. The thorax joint reaches a maximum angle of  $0.06 \pm 0.01$  rad in the middle of the finger depression phase of the key, and returns to a zero angle at the end of the attack after  $0.68 \pm 0.02$  sec. The articulation of the thorax in abduction(-)/adduction(+), in external rotation (-)/internal (+) and in extension(-)/flexion(+) of the humerus remains within an interval of  $0.25 \pm 0.05$  rad throughout the movement. The ulna, during the first phase of the attack, varies by an angle of  $0.1 \pm 0.2$  rad in extension, to return from the end of the contact phase, in flexion, to the initial angle. The radius hardly changes throughout the simulation. While the articular angle of the hand hardly varies throughout the movement (within 0.1 rad) during the descent phase in the fingerboard, the hand varies by an angle of  $0.4 \pm 0.1$  rad in flexion. The joint angle of the index finger varies in extension throughout the first phase by  $0.3 \pm 0.1$  rad, and, by a sudden flexion movement, increases steeply by an angle of  $1 \pm 0.1$  rad from the moment he begins to press the key. At the moment of the contact phase, the index finger varies in an interval of 0.5 rad in flexion, then in extension, before leaving the touch with a variation in articular angle of only  $0.2 \pm 0.05$  rad. The joint velocities in radians per second of the same degrees of freedom as a function of time are presented in Appendix K.

Still for each of these 10 degrees of freedom, Figure 25 below shows in orange their joint torque in Nm as a function of time (s). The joint torques of the pelvis in anteversion, of the thorax in right rotation, in flexion and of the humerus in adduction, in external rotation and in flexion, vary within an interval of  $5 \pm 0.5$  Nm. The joint torque of the ulna in flexion remains on average at a value of 1 Nm throughout the first, then in extension, when the finger comes into



contact with the bottom of the key, reaches a peak of  $5 \pm 0.5$  Nm. During the phase of finger contact with the bottom of the key, the torque of the ulna in flexion reaches a new peak of  $4 \pm 0.5$  Nm, before returning to zero torque at the end of the attack. The torque of the radius varies between  $-1$  and  $1 \pm 0.2$  Nm at the moment of the descent of the key, but remains zero throughout the first and last phase of the attack. The joint torques of the hand and the index also remain zero throughout the movement, except when the finger comes into contact with the bottom of the key, where the torque of the hand which is in extension reaches a value of  $5$  Nm and where the torque of the finger which is in flexion reaches a value of  $2.5 \pm 0.2$  Nm.

Figure 23 below represents the contact forces, along the 3 axes, present during the contact between the tip of the index finger and the bottom of the piano key when playing the key. These contact forces vary from  $0$  to  $5 \pm 0.5$  N in X, from  $-5$  to  $0.1 \pm 0.02$  in Y, and from  $0$  to  $30 \pm 1$  N in Z.

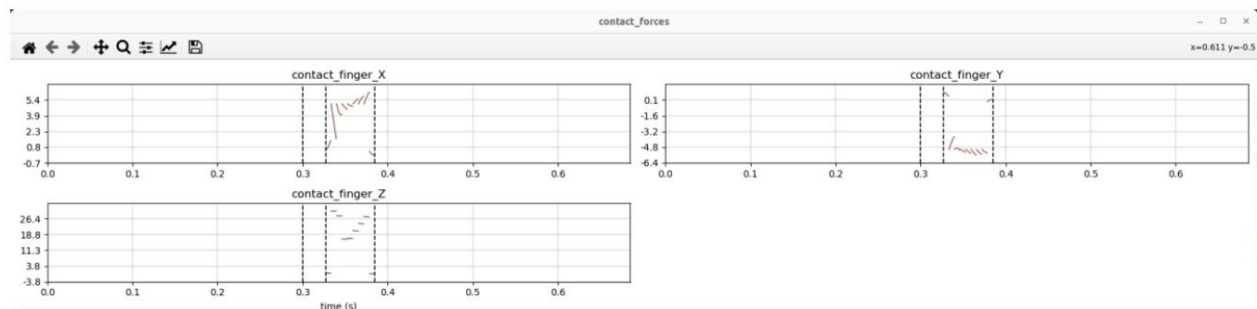


Figure 23: Contact forces (in N) of the 3 axes of the finger at the bottom of the key as a function of time (s).

### Animation of the solution

The animation of this specific kinematic solution thus represents the skeletal model of a pianist playing the game of an LA in staccato hit attack, with an imposed minimization weight equal to all the joints.

It can be viewed on the following links: Front view:

<https://drive.google.com/file/d/1RII14CZ8cMxbdS9TQC-74f9rrdSt5sY9/view> Side view: [https://drive.google.com/file/d/1qx4QZ8I3X0RR4khkXL\\_-cMB4kgHWdj12/view](https://drive.google.com/file/d/1qx4QZ8I3X0RR4khkXL_-cMB4kgHWdj12/view)

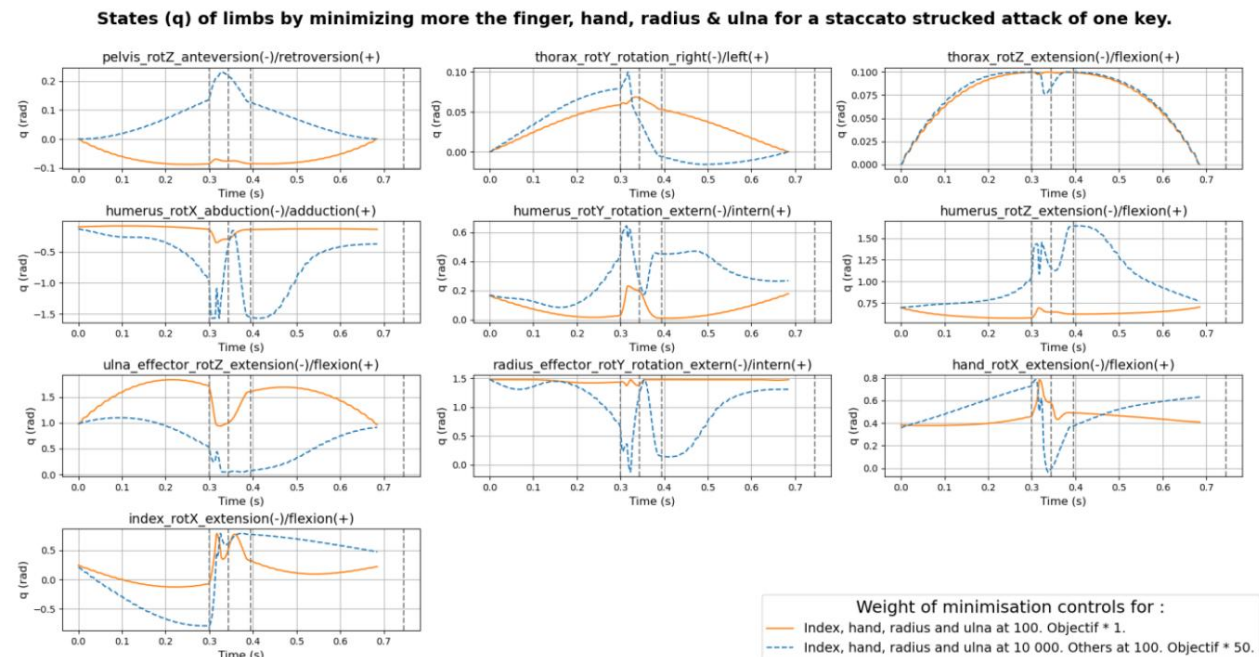


Figure 24: Joint positions (in rad) of the 10 degrees of freedom of the model as a function of time (s) for two different simulations of a slap game.

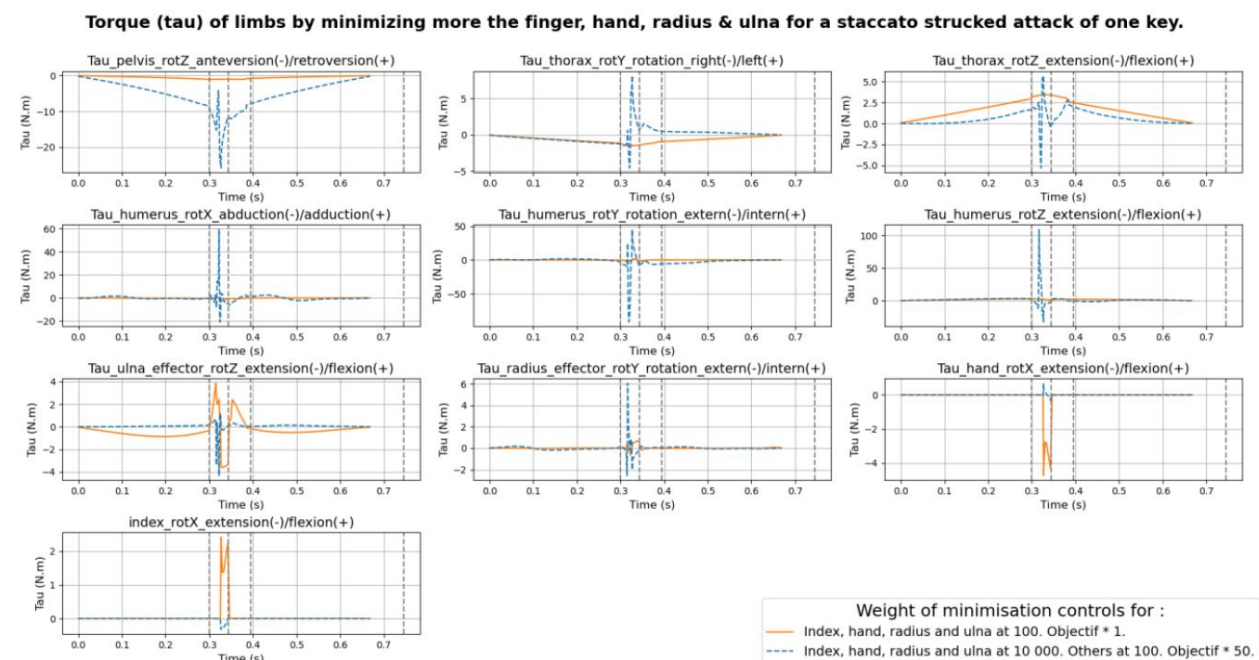


Figure 25: Joint torques (in Nm) of the 10 degrees of freedom of the model as a function of time (s) for two different simulations of a slap game.

### 3. 2. Kinematic solution minimizing upper body distal joints for a game hit staccato

For the ~~particular kinematic simulation carried out for~~ a staccato hit game ~~minimizing in priority the~~ torques of the distal joints of the upper body, an optimal solution has been found. The program took 505.866 seconds to find this controlled optimal solution (see Appendix I) with 212 iterations.

The total sum of the costs of his objectives is  $8.147 \times 10^5$  (size of an objective = weight\*values). The main data of the optimal kinematic solution found as a function of time are displayed in Figure 24, Figure 25, and Figure 26. Each phase of the simulation is delimited by a vertical dotted line.

First of all, Figure 24 above shows in blue the joint position in radians of each of the 10 degrees of freedom of the model of this simulation. It can be observed that the articular angle of the pelvis reaches a peak by retroversion of  $0.22 \pm 0.1$  rad while the finger sinks into the key, just before the contact phase, i.e. at  $0.33 \pm 0.02$  sec, before leaving to its original position by anteversion. The angle of the thorax joint reached by a rotation to the left  $0.1$  radian during the descent phase in the key, just before performing a rotation to the right by an angle of  $0.15 \pm 0.02$  rad. During the descent of the finger inside the fingerboard, the articular angle of the humerus varies by adduction of an angle difference of  $1.5 \pm 0.1$  rad, by internal rotation of  $0.45 \pm 0.02$  rad and by flexion of  $0.3 \pm 0.02$  rad in an interval of  $0.02 \pm 0.01$  sec. The ulna joint evolves in extension throughout the first phase in an angle difference of  $1 \pm 0.2$  rad and then ends the attack with a movement of flexion returning to its initial position located at therefore  $1 \pm 0.2$  rad. At the moment of the descent of the finger into the key, the articulation of the radius reaches a first peak of  $1.5 \pm 0.2$  rad by internal rotation, and a second at the end of the phase of contact of the finger at the bottom of the key of  $1 \pm 0.2$  rad, before returning to its initial angle at  $1.3$  radian by external rotation. During the first phase, the articular angle of the hand varies by  $0.4 \pm 0.02$  rad per flexion, before reaching a peak of  $0.8 \pm 0.02$  rad per extension during the key depression phase. At the moment of contact of the finger at the bottom of the key, the articulation of the hand varies by bending through an angle of  $0.4 \pm 0.02$  rad, before finally leaving the key with an angle variation of  $0.2 \pm 0.02$  rad. The joint angle of the index finger varies in extension throughout the first phase by  $0.9 \pm 0.02$  rad, and by a movement of flexion increases steeply by an angle of  $2 \pm 0.1$  rad from the time it begins to press the key, to finally stay at the same position within  $0.4 \pm 0.02$  rad. The joint velocities in radians per second of the same degrees of freedom as a function of time are presented in Appendix K.

Still for each of these 10 degrees of freedom, Figure 24 above shows in blue their joint torque is displayed in Newton meters as a function of time in seconds. It can be observed there that when the articular torque of the pelvis in anteversion evolves in an interval of  $5 \pm 0.2$  Nm throughout the attack, except when the finger comes into contact with the bottom of the key where the torque of the pelvis in anteversion always reaches a peak of  $-30 \pm 1$  Nm. The torque of the thorax joint in right rotation reaches a peak of  $5 \pm 0.2$  Nm just during the descent of the key, and this torque of the thorax but in left rotation this time reaches a new peak of  $10 \pm 0.5$  Nm at the moment of contact of the finger with the bottom of the key. The torque of the thorax joint in flexion gradually increases until it reaches  $5 \pm 0.2$  Nm when the finger comes into contact with the key, goes down to a zero value then goes up one last time reaching a peak twice as large, of  $10 \pm 1$  Nm, before

to finally come down to zero torque. Throughout the 1st and last phase, the joint torque of the humerus in abduction/adduction remains at an average value of  $5 \pm 0.2$  Nm, that of the humerus in external/internal rotation remains at an average value of  $10 \pm 5$  Nm, the joint torque of the humerus in extension/flexion at an average value of  $2 \pm 1$  Nm, that of the ulna in extension/flexion also at an average value of  $0.05 \pm 0.01$  Nm, of the radius of  $0.01 \pm 0.01$  Nm, and the joint torques of the wrist and index finger remain at a zero value. Just before the finger comes into contact with the bottom of the key, the joint torque of the humerus in adduction reaches a peak of  $41 \pm 1$  Nm, the torque of the humerus joint in external rotation reaches a peak of 60 Nm, that of the humerus in flexion reaches a peak of  $30 \pm 1$  Nm, that of the ulna in extension a peak of  $5 \pm 0.1$  Nm and that of the radius in internal rotation a peak of  $1.2 \pm 0.2$  Nm. And finally, when the finger comes into contact with the bottom of the key, the joint torque of the humerus in internal rotation reaches a peak of  $20 \pm 1$  Nm, that of the humerus in extension a peak of  $20 \pm 1$  Nm, the joint torque of the radius in external rotation reaches a peak of  $1.2 \pm 0.2$  Nm, that of the wrist in flexion a peak of  $0.01 \pm 0.01$  Nm, and finally the torque of the wrist in extension reaches a torque of  $0.01 \pm 0.01$  Nm.

Figure 26 below represents the contact forces, along the 3 axes, present during the contact between the tip of the index finger and the bottom of the piano key when playing the key. These forces of contact vary from  $-4$  to  $0 \pm 0.5$  N in X, from  $-5$  to  $\pm 5$  in Y, and remains zero at  $\pm 1$  N in Z.

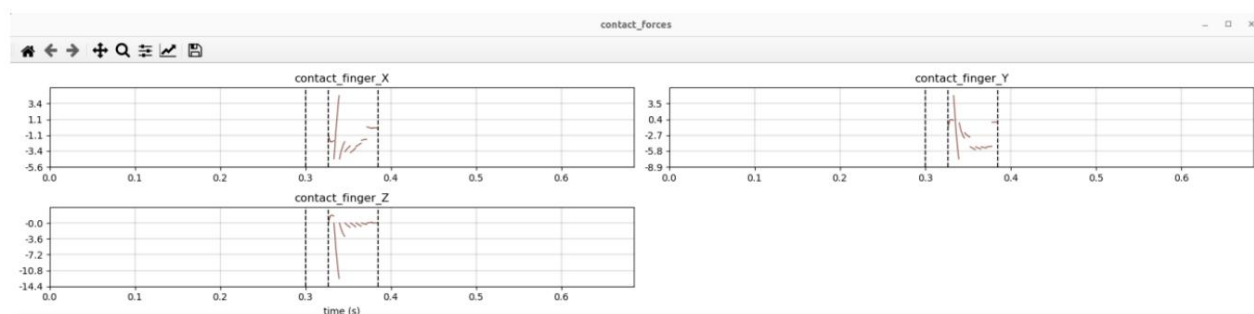


Figure 26: Contact forces (in N) of the 3 axes of the finger at the bottom of the key as a function of time (s).

### Animation of the solution

The animation of this specific kinematic solution thus represents the skeletal model of a pianist playing the game of an LA in attack struck staccato, with a large minimization weight imposed on the 4 distal joints of the upper body, in other words the finger, wrist, radius and ulna.

It can be viewed on the following links: Front view: [https://drive.google.com/file/d/14CQShM7nqtJAomYao96DI-5\\_-BoFp6y/view](https://drive.google.com/file/d/14CQShM7nqtJAomYao96DI-5_-BoFp6y/view)

Side view: [https://drive.google.com/file/d/13F\\_2QvLG9gJbh3FYhVxCNfal\\_c5ZbWqJ8/view](https://drive.google.com/file/d/13F_2QvLG9gJbh3FYhVxCNfal_c5ZbWqJ8/view)

## 4/ Discussion

The objective of this study project is to find numerically a kinematic piano strategy minimizing the use of distal joints for the simulation of simple piano tasks, in order to reduce exposure to the risk of musculoskeletal disorders related to instrumental practice.

The use of optimal control allowed to develop two kinematic solutions minimizing more or less the distal members of the model, for a key attack in staccato pressed game, then for an attack in staccato hit game.

### **4. 1. Commentary and discussion on the staccato pressed stops obtained.**

#### **¶ 4. 1. 1. Commentary on the benchmark solution obtained for a staccato hurried game**

As a reminder, this benchmark solution for a staccato hurried game minimizes each of the joint couples of the model as much to a weight of 100, so it does not prioritize any couple more than another.

- Throughout the attack, the joint angle of the pelvis and the thorax only varies by an angle of  $0.1 \pm 0.05$  rad and their joint torque only varies within an interval of  $3 \pm 0.5$  Nm. articulation of the ulna evolves throughout the attack, and more particularly at the moment of the release of the key, by an angle of  $1.1 \pm 0.2$  rad, and its articular torque reached 4 Nm both in extension and in bending. The joints of the hand and the finger are also used throughout the attack, and more particularly when the finger comes into contact with the bottom of the fingerboard.

Their articular angles evolve respectively  $0.9 \pm 0.02$  rad and  $0.4 \pm 0.2$  rad, and their torques respectively reach a peak of 5 Nm in extension for the hand, and a peak of  $2.5 \pm 0.5$  Nm at the moment of contact of the finger to the bottom of the key. It can be concluded that the model mainly uses its distal limbs, more particularly the ulna, the wrist and the finger, the ulna being the most mobilized joint. His proximal limbs, and more particularly his pelvis and thorax, are very little mobilized.

- When pressing the key, it can be noticed visually on the animation, as well as on Figure 20 displaying the articular positions of the wrist, that the pianist model performs a movement with the wrist which seems quite realistic. During the descent of the finger in the fingerboard, the wrist performs an angle flexion of  $0.6 \pm 0.02$  rad, due to the resistance of the fingerboard on the finger modeled in our case by a velocity profile imposed throughout the descent in the key. Just after the phase of contact of the finger at the bottom of the key, the hand starts from it again making a small flexion of  $0.8 \pm 0.05$  rad to compensate for the rapid attack of the note aided by the imposition of an impact on the bottom of the key. This kinematics of the hand found in this simulation is realistic and can be found in real conditions in the game of an attacked key (Furuya et al. 2010).

- Finally, it can be observed on the graph displaying the contact forces of the key applied to the finger (Figure 19), that the force applied to the finger along the Z axis reaches a value of  $30 \pm 1$  N, a consistent value because similar to that found in Gillespie's article (Gillespie et al. 2011).

#### **4. 1. 2. Commentary on the solution minimizing upper body distal joints for a rushed staccato game.**

As a reminder, this solution found for a staccato hurried game further minimizes the distal joints of the upper body, with a weight equal to 10,000, that is to say 100 times greater than the proximal joints of the upper body.

Indeed, despite the fact that the joint angles of the hand and the finger vary throughout the movement respectively in an interval of  $0.8 \pm 0.02$  rad, and  $0.5 \pm 0.02$  rad on average (Figure 20), their joint torques are zero (Figure 21). The joints that compensate for this lack of torque on the distal joints are the pelvis in anteversion which has a joint torque of up to  $30 \pm 1$  Nm, the thorax in left rotation which has a torque varying within an interval of  $15 \pm 1$  Nm, the thorax in flexion reaching a torque of  $10 \pm 0.5$  Nm, the humerus in adduction reaching a torque of up to  $42 \pm 1$  Nm, the humerus in external rotation reaching a torque of  $-60 \pm 2$  Nm, and finally the humerus in extension and flexion reaching a joint torque of up to  $22 \pm 1$  Nm. Most of the torques mentioned above reach their maximum value in the middle of the attack, when the finger comes into contact with the bottom of the key. Visually, it can be observed on the animation that the retroversion of the pelvis, and the humerus in abduction/adduction and extension/flexion allows the ulna and the hand to have an articular angle which does not vary (at 0.2 radians, Figure 20) with the aim of minimizing their joint torque throughout the first phase in particular (Figure 21). Verdugo et al. 2020 documented an anteversion movement of the pelvis when attacking a touch in pressed and struck play. The simulation developed within the framework of this internship is thus interesting, because it shows that the anteversion of the pelvis can also be used to reduce the load imposed on the distal joints.

Finally, it can be observed on the graph displaying the contact forces of the key applied to the finger (Figure 22) that the force, applied to the finger along the Z axis, reached remains at a zero value to within 0.1 N. However, the forces applied in X and Y reach a value of  $-5 \pm 0.2$  N.

The values of these forces mean that the model attacks the piano key with a significant movement going forwards, and towards the side of the key, and an almost null vertical movement. On the animation, it can be seen that the pelvis goes from a retroversion to an anteversion in less than  $0.1 \pm 0.2$  s when the finger comes into contact with the bottom of the key, which carries the finger and the hand forward of the note just after the contact phase.

#### **4. 1. 3. Comparison of the two solutions obtained for a pressed staccato game**

At the time of the first phase, when the finger is in contact with the key, on the solution further minimizing the distal joints of the model, the pelvis achieves a certain anteversion of  $0.25 \pm 0.02$  rad in order to minimize the joint torque of the distal joints in the continuation of the movement, contrary to the initial reference solution which keeps the pelvis in an articular angle of  $0.1 \pm 0.02$  rad only. At the time of the descent phase of the key, for the reference solution, the joint torque of the 3 degrees of freedom of the humerus remains zero while the joint torque of the ulna in extension varies by  $6 \pm 0.5$  Nm. , at the time of this same phase for the solution minimizing the torques of the distal joints, the joint torque of the humerus in adduction reaches a peak of  $40 \pm 1$  Nm, that of the humerus in external rotation a peak of  $60 \pm 1$  Nm and that of the humerus in flexion a

peak of  $30 \pm 1$  Nm, while the joint torque of the hand and the finger remains zero, and that of the ulna evolves in a smaller interval of  $2.2 \pm 0.2$  Nm. When the finger comes into contact with the bottom of the touch, the force imposed by the touch on the finger reaches a value of  $30 \pm 1$  N in Z for the reference solution, and the hand and the finger react to this force by the evolution of their articular angle of  $0.35 \pm 0.05$  rad in flexion for the hand, and  $0.8 \pm 0.5$  rad in extension for the finger. On the contrary, in the particular solution found, the force imposed by the touch on the finger is zero in Z, but  $5 \pm 0.2$  N in X and Y. The hand and the finger do not react (change in their articular angle null), it is mainly the pelvis which returns to its initial null position (by the evolution of its angle of  $0.25 \pm 0.02$  rad), and the humerus with its three degrees of freedom, which thus make the finger start again from the key, and which repositions the model to its initial position.

## 4. 2. Commentary and discussion on the staccato hits obtained

### 4. 2. 1. Commentary on the benchmark solution obtained for a staccato hit game

As a reminder, the first solution found for a staccato hit game is a solution that minimizes each of the joint couples of the model to a weight of 100, so it does not prioritize any couple more than another.

- Throughout the attack, the articular angle of the pelvis and the thorax only varies by an angle of  $0.1 \pm 0.03$  rad, and their joint torque only varies within an interval of  $3 \pm 0.2$  rad. The joint torques of the 3 degrees of freedom of the humerus are also zero throughout the simulation. Conversely, the ulna joint evolves throughout the attack, by an angle of  $2 \pm 0.1$  rad, and its joint torque reaches 4 Nm both in extension and in flexion at the time of the descent of the the key and the contact phase of the finger at the bottom of the key. The joints of the hand and the finger are also well used throughout the attack and particularly during the 2nd and 3rd phase. Their joint angles both reach a peak at  $0.8 \pm 0.02$  rad at  $0.32 \pm 0.02$  s at the moment the key sinks for the hand and the finger, and also in the middle of the key descent phase for the finger joint. At the same instants, their joint torques respectively reach a peak at  $4.2 \pm 0.2$  Nm in extension for the hand, and a peak at  $2.2 \pm 0.2$  Nm for the finger in flexion, while the joint torques of certain distal limbs remain zero. It can be concluded that the model mainly uses its distal limbs, more particularly the ulna, the wrist and the finger, the ulna being the most mobilized joint. Verdugo et al. 2020 shows the same results, also claiming that the elbow is the main culprit for the descent of the key. His proximal limbs, and more particularly his pelvis and thorax, are very little mobilized.

- During the attack inside the key, it can be noticed visually on the animation, as well as on Figure 24 displaying the articular positions of the wrist, that the pianist model realizes a movement with the wrist which seems quite fact realistic. During the descent of the finger in the fingerboard, the wrist achieves an angle extension of  $0.8 \pm 0.02$  rad, due to the resistance of the fingerboard on the finger modeled in our case by a velocity profile imposed throughout the descent in the key. During the contact phase, the hand performs a small extension then flexion of  $0.1 \pm 0.05$  rad, and the finger a small flexion then extension of  $0.45 \pm 0.1$  rad, before leaving the key by making the hand a small progressive extension of  $0.1 \pm 0.05$  rad, and for the finger a flexion progresses until the end of the last

phase, and this, to compensate for the fast attack of the key helped by the imposition of an impact at the bottom of the key. This kinematics of the hand found in this simulation is realistic and can be found in real conditions in the game of an attacked key (Furuya et al. 2010).

Finally, it can be observed on the graph displaying the contact forces of the key applied to the finger (Figure 23), that the force applied to the finger along the Z axis reaches a value of  $30 \pm 1$  N, similar to that found in Gillespie's article (Gillespie et al. 2011).

#### ¶ 4. 2. 2. Commentary on the solution minimizing upper body distal joints for a staccato hit game.

As a reminder, the second solution found for a staccato hit game further minimizes the upper body's distal joints, with a weight equal to 10,000, that is to say 100 times greater than the upper body's proximal joints.

Indeed, despite the fact that the joint angles of the hand and the finger vary throughout the movement respectively in an interval of  $0.8 \pm 0.02$  rad, and  $1.8 \pm 0.1$  rad on average (Figure 24), their joint torques are zero to within  $0.2 \pm 0.05$  Nm (Figure 25). The joints that compensate for this lack of torque on the distal joints are the pelvis in anteversion which has a joint torque of up to  $29 \pm 1$  Nm, the thorax in left rotation which has a torque varying within an interval of  $13 \pm 1$  Nm, the thorax in flexion and in extension reaching a torque of  $11 \pm 1$  Nm, the humerus in adduction reaching a torque of up to  $60 \pm 1$  Nm, the humerus in external rotation reaching a torque of  $90 \pm 5$  Nm, and finally of the humerus in flexion reaching a joint torque of up to  $110 \pm 10$  Nm. The majority of the torques mentioned above reach their maximum value in the middle of the descent of the finger into the fingerboard. Visually, it can be observed on the animation that the retroversion of the pelvis, and of the humerus in abduction/adduction and extension/flexion allows the ulna to have an articular angle which varies very little (in a interval of 0.1 rad) in order to minimize their joint torque throughout the first phase in particular. However, still on the animation, during the first phase of the attack, it can be noticed that the finger performs an extension movement (of  $0.4 \pm 0.02$  rad, Figure 24). The finger thus behaves to minimize the distal joint torques, while continuing to follow the speed profile imposed on it when the key is pressed. This extension allows him to gain momentum before playing the note.

Finally, it can be observed on the graph displaying the contact forces of the key applied to the finger (Figure 26) that the force reached, applied to the finger along the Z axis, remains at a zero value to within 0.1 N. However, the forces applied in X and Y reach a value of  $5 \pm 0.2$  N.

The values of these forces mean that the model attacks the piano key with a large movement going forwards, and towards the side of the key, and almost zero movement vertically.

On the animation, it can be seen that the pelvis goes from a retroversion to an anteversion in less than  $0.1 \pm 0.2$  s (Figure 24) when the finger comes into contact with the bottom of the key, which carries the finger and hand forward of the note just after the contact phase.



#### 4. 2. 3. Comparison of the two solutions obtained for a staccato hit game

At the time of the first phase, when the hand is at a certain distance from the fingerboard, on the solution further minimizing the distal joints of the model, the pelvis realizes a certain retroversion of  $0.25 \pm 0.1$  rad (Figure 24) in order to minimize the joint torque of the distal joints throughout the movement. Conversely, the initial benchmark solution keeps the pelvis in anteversion at a small articular angle of only  $0.1 \pm 0.02$  rad. At the time of the descent phase of the touch, for the reference solution, the joint torque of the 3 degrees of freedom of the humerus remains zero while the joint torque of the ulna in extension varies by  $8 \pm 0.5$  Nm. , at the time of this same phase for the solution minimizing the torques of the distal joints, the joint torque of the humerus in adduction reaches a peak of  $60 \pm 1$  Nm, that of the humerus in external rotation reaches a peak of  $90 \pm 5$  Nm and of the humerus in flexion a peak of  $110 \pm 1$  Nm, while the joint torque of the hand and finger remains zero, and that of the ulna evolves in a smaller interval of  $4 \pm 0.2$  Nm. When the finger comes into contact with the bottom of the key, the force imposed by the key on the finger reaches a value of  $30 \pm 1$  N in Z for the reference solution, and the hand and the finger react to this force by evolution of their articular angle of  $0.4 \pm 0.02$  rad in flexion for the hand, and of  $1 \pm 0.5$  rad in flexion for the finger.

On the contrary, in the particular solution found, the force imposed by the key on the finger is zero in Z, and only  $5 \pm 0.2$  N in X and Y. The hand therefore does not leave the key by a vertical movement powerful, but by a small longitudinal and forward movement in relation to the key, before returning to its initial position.

# Conclusion

## 1/ Technical conclusion

To conclude, this study has shown, by numerical analysis thanks to optimal control, that for a simple piano playing in pressed attack or struck staccato, it is indeed the joints of the ulna, the wrist, as well as the finger in extension. /flexion which are the most used. Their joint angular variations, as well as their respective joint torques, are much greater than those of the proximal joints. These results are consistent with the importance of distal joints in piano playing documented in the literature, as well as with the high risk of onset of musculoskeletal disorders in the distal body segments of pianists (particularly at the elbow and wrist). . A second numerical analysis was then able to show that for a piano game minimizing the joint torques of the distal limbs, it is the joints of the pelvis in retroversion/anteversion and of the humerus under its three degrees of freedom which are the most mobilized. throughout the attack. The variation of their angles and their joint torques is in this case much greater than that of the distal joints. The minimization of the distal articular torques nevertheless maintains respect for the criteria which distinguish a hurried game from a struck game, being the speed of descent of the finger during the attack, and the time spent by the finger at the bottom of the key . This differentiation, thus respected in this second analysis, is important for successfully adapting to the wide variety of musical contexts found in the piano repertoire.

## 2/ Personal conclusion

From a technical point of view, this internship brought me a lot. I discovered the optimal control theory, which I was able to put into practice thanks to the *Bioptim python library*. I was able to develop my skills in python programming, as well as in data analysis. In addition, I discovered the world of research by carrying out this study. I acquired skills in scientific writing, both in terms of text structure and the expected writing style.

From a social point of view, this internship taught me to work with a team of students and researchers. The weekly meetings taught me to synthesize the ideas to present at each meeting, to structure my study follow-up, as well as to target my questions in order to facilitate my work autonomy until the next meeting.

Finally, this internship allowed me to discover a new country, as well as a new continent, the Canada of America. I really enjoyed discovering the local population who are particularly attentive to others, and I loved getting lost in the many national parks that wood this city of Montreal.

# Bibliography

- Bragge, Peter, Andrea Bialocerkowski, and Joan McMeeken. 2006. "A Systematic Review of Prevalence and Risk Factors Associated with Playing-Related Musculoskeletal Disorders in Pianists." *Occupational Medicine (Oxford, England)* 56 (1): 28-38. <https://doi.org/10.1093/occmed/kqi177>.
- Furuya, Shinichi, and Eckart Altenmüller. 2013. "Flexibility of movement organization in piano in 7. performance ". *Frontiers human Neuroscience* <https://www.frontiersin.org/articles/10.3389/fnhum.2013.00173>.
- Furuya, Shinichi, Eckart Altenmüller, Haruhiro Katayose, and Hiroshi Kinoshita. 2010. "Control of multi joint arm movements for the manipulation of touch in keystroke by expert pianists". *BMC Neuroscience* 11. <https://doi.org/10.1186/1471-2202-11-82>.
- Gillespie, R. Brent, Bo Yu, Robert Grijalva, and Shorya Awtar. 2011. "Characterizing the Feel of the Piano Stock ". *Computer Music Journal* 35 (1): 43-57.
- Goebel, Werner, Roberto Bresin, and Alexander Galembo. 2005. "Touch and temporal behavior of grand piano actions". *The Journal of the Acoustical Society of America* 118 (September): 1154-65. <https://doi.org/10.1121/1.1944648>.
- Goebel, Werner, and Caroline Palmer. 2008. "Tactile Feedback and Timing Accuracy in Piano Performance." *Experimental Brain Research* 186(3): 471-79. <https://doi.org/10.1007/s00221-007-1252-1>.
- Kaur, Jaspreet, and Sandeep Singh. 2016. "NEUROMUSCULOSKELETAL PROBLEMS OF UPPER EXTREMITIES IN MUSICIANS-A LITERATURE REVIEW." *International Journal of Therapies and Rehabilitation Research* 5 (January): 14. <https://doi.org/10.5455/ijtrr.000000120>.
- Kinoshita, Hiroshi, Shinichi Furuya, Tomoko Aoki, and Eckart Altenmüller. 2007. "Loudness control in pianists as exemplified in keystroke force measurements on different keys". *The Journal of the Acoustical Society of America* 121 (5): 2959-69. <https://doi.org/10.1121/1.2717493>.
- "True\_Pianoptim". (2021) 2022. Python. s2mLab. <https://github.com/s2mLab/PianOptim>.
- Verdugo, Felipe, Justine Pelletier, Benjamin Michaud, Caroline Traube, and Mickaël Begon. 2020. "Effects of Trunk Motion, Touch, and Articulation on Upper-Limb Velocities and on Joint Contribution to Endpoint Velocities During the Production of Loud Piano Tones." *Frontiers in Psychology* 11:1159. <https://doi.org/10.3389/fpsyg.2020.01159>.


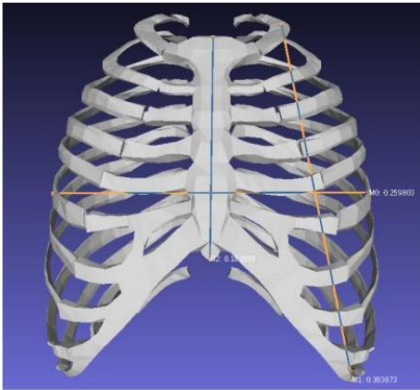
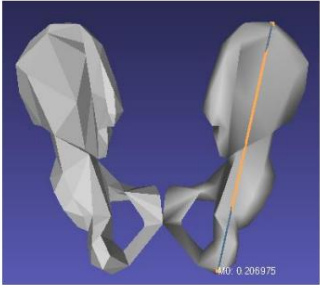
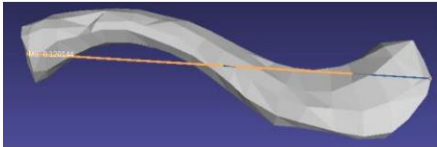
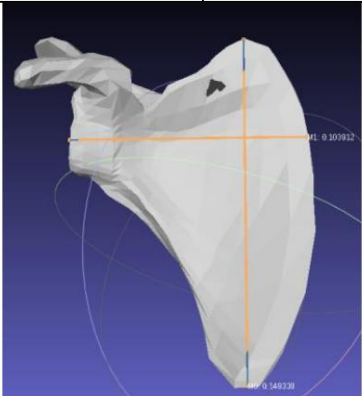

## Appendix A: Libraries and python functions used



```
from casadi import MX, acos, vertcat, dot, pi
import time
import numpy as np
from matplotlib import pyplot as plt
from numpy import ndarray
import biorbd_casadi as biorbd
import pickle
from pickle import dump
from bioptim import (
    PenaltyNode,
    ObjectiveList,
    PhaseTransitionFcn,
    DynamicsList,
    ConstraintFcn,
    BoundsList,
    InitialGuessList,
    CostType,
    PlotType,
    PhaseTransitionList,
    Node,
    OptimalControlProgram,
    DynamicsFcn,
    ObjectiveFcn,
    ConstraintList,
    PenaltyNodeList,
    QAndQDotBounds,
    OdeSolver,
    BiorbdInterface,
    Solver,
    Axis
)
```




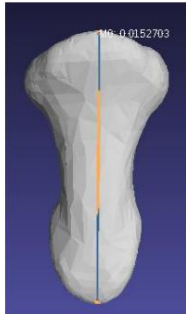
**Figure Annex - 1 :** Imports of libraries and python functions used

## Appendix B: Model Bone Dimensions

### 3d skeleton

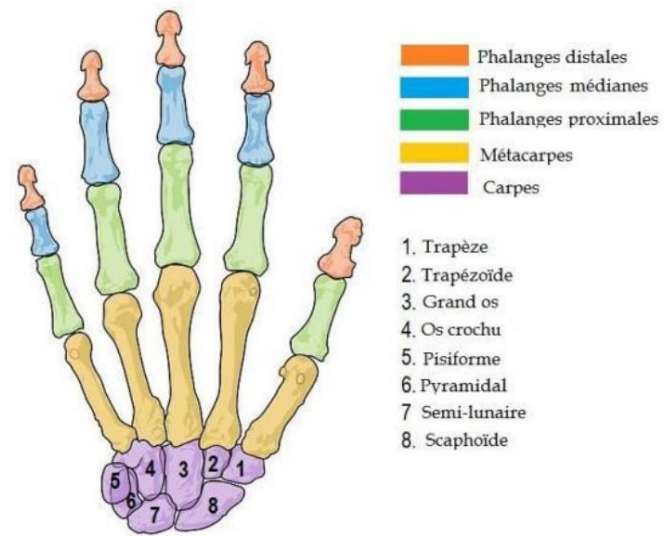
Upper body					
Spine		Thorax			Bowl
Height	Width	Height of the Center	Diagonal	Width	Height
0.5124m	0.0618m	0.1838m	0.3088m	0.2598m	0.2069m
					
Clavicle		Scapula		Humerus	
Length		Height	Width	Height	Width
0.1201m		0.1493m	0.1039m	0.316m	0.020m
					

Radius		Ulna	
Height		Height	
0.2370m		0.2588m	
			

Hand (see Appendix C)			
Metacarpus 2	Proximal phalanx 2	Intermediate phalanx 2	Distal phalanx 2
Height	Height	Height	Height
0.058111m	0.038358m	0.022435m	0.015270m
			

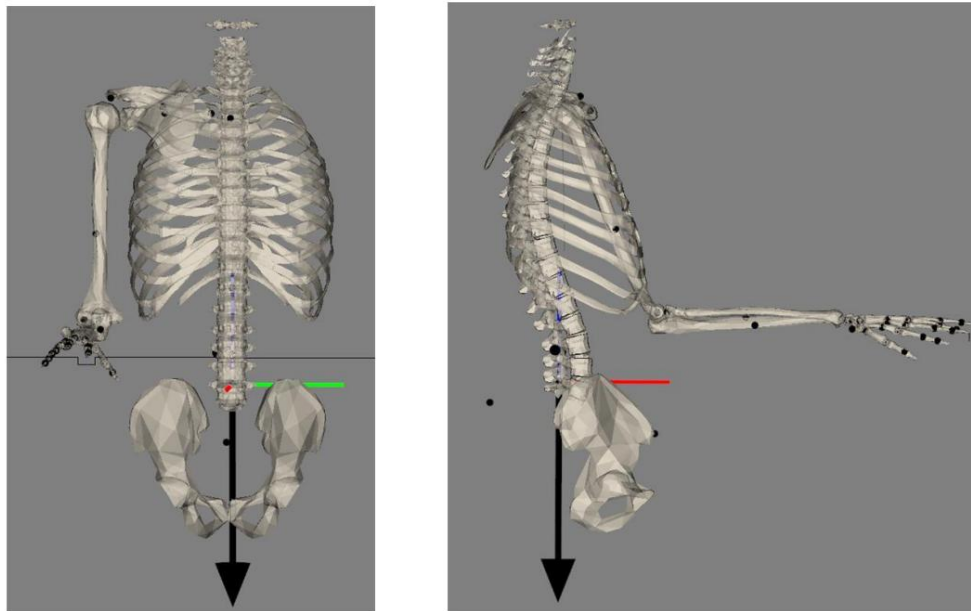
**Figure Appendix - 2:** Dimensions of the bones used in the model from the WU and Stanford model.

## Appendix C: Hand Bones



**Figure Appendix - 3:** Skeleton of hand bones and their names.

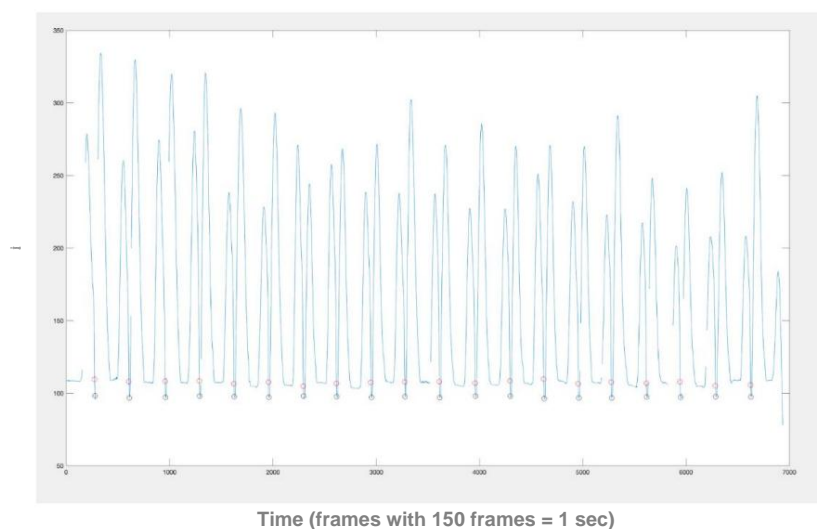
## Appendix D: Initial Skeleton Position



**Figure Appendix - 4:** Initial position of the joint couples throughout the simulation, unrelated to the displayed position of the model at the first node of the animation.

## Appendix E: Special study on the speed profiles of a hitting and pressing game

A few months ago Felipe Verdugo made an experimental take where he partly recovered by motion capture the piano gesture of a pianist playing an A of the main octave in staccato hit touch, then in staccato pressed touch. The pianist was equipped with reflective sensors all over his body and played on a piano surrounded by *Vicon* infrared cameras which made it possible to recover frame by frame (150 frames = 1 second) the exact positions of each sensor in space. All the data has thus been recovered in a .c3d file, and it is thanks to the "Vicon Nexus" software, which displays the pianist playing, that it is possible to recover the exact frame where the finger of each of the 20 attacks is landed on the sidelines, and the frame where it hits the bottom of the sidelines. It has been observed that the finger takes on average, for a staccato hit game, 6 seconds to descend inside the key, and that it spends on average 9 seconds at the bottom of the key. Also, by taking the average of the difference in position between each frame of these 20 attacks during the phase where the finger is descending, it is thus possible to calculate the average velocity profile during the descent of the finger in the key during a tapped staccato game, then during a pressed staccato game. The speed profiles below (Appendix Figure - 5) were respectively obtained for a struck staccato, and for a pressed staccato playing, for the attack of 20 notes, and it is from these profiles that the two profiles Mean speeds of the 20 attacks during the descent phase into the key have been plotted respectively (Figure Appendix – 6). It is thus these two average speed profiles that will be used for the simulation.



*Figure Appendix - 5 : Position of the tip of the index finger in relation to time for the game of 20 attacks struck staccato*



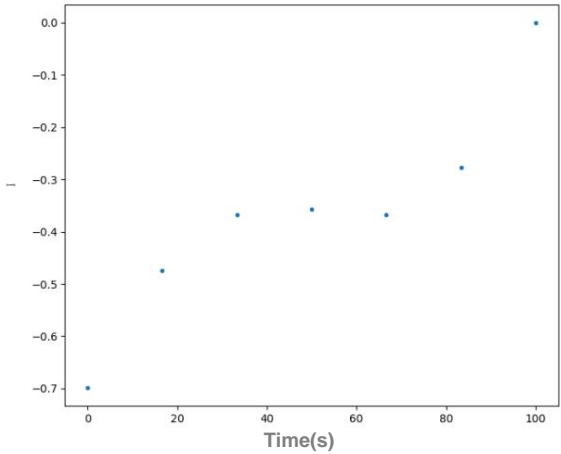


Figure Annex – 6: Average speed profile of the finger during its descent into the key in play struck

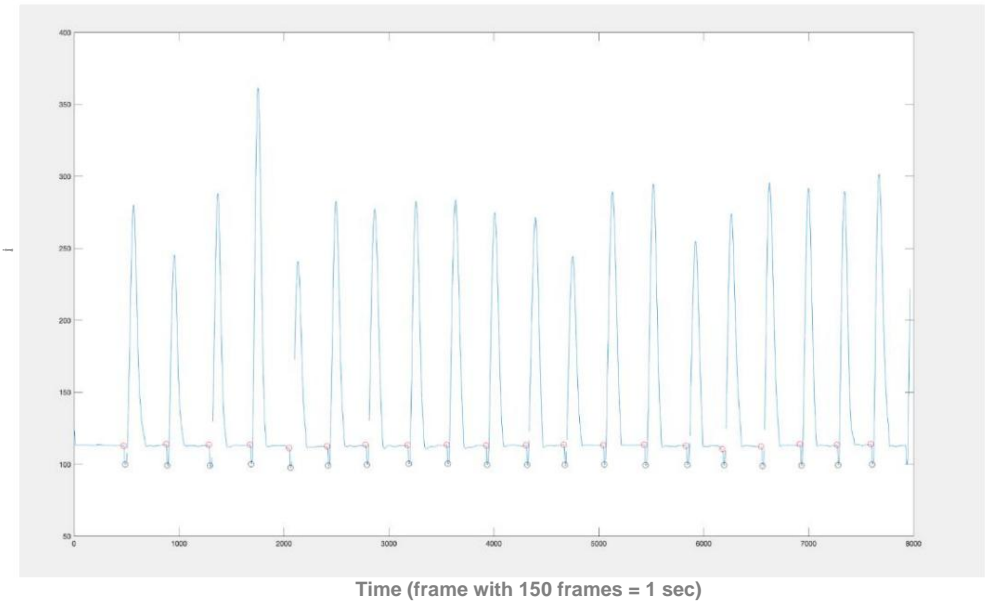


Figure Appendix – 5 bis : Position of the tip of the index finger in relation to time for the game of 20 staccato pressed attacks

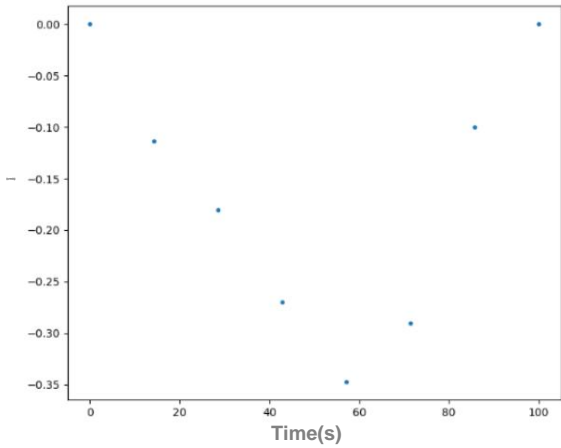
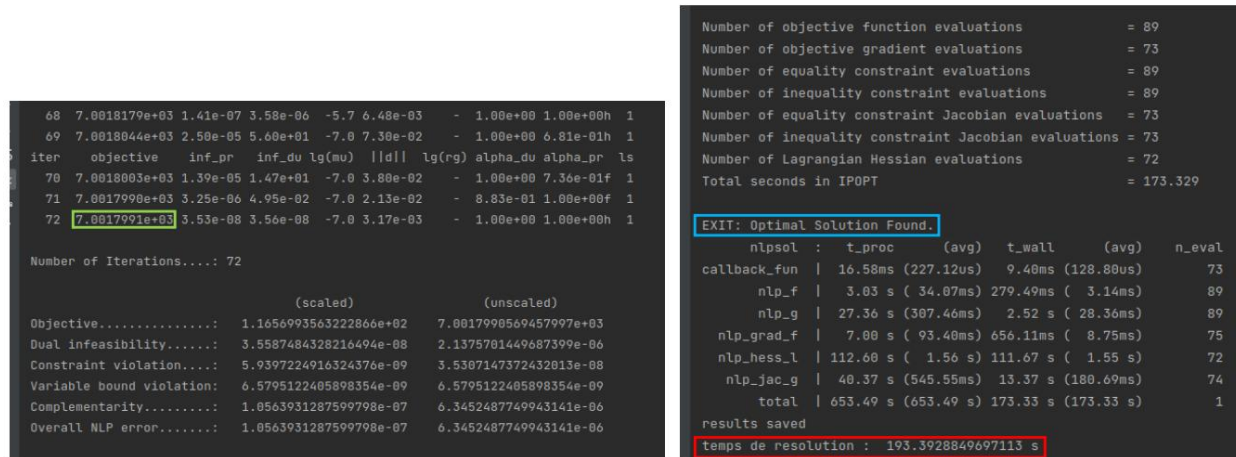


Figure Annex – 6 bis: Average speed profile of the finger during its descent into the key in play pressed

# Appendix F: Optimal Solution found 1



**Figure Appendix - 7:** Optimal solution found by the program for a staccato hurried game without any particular minimization.

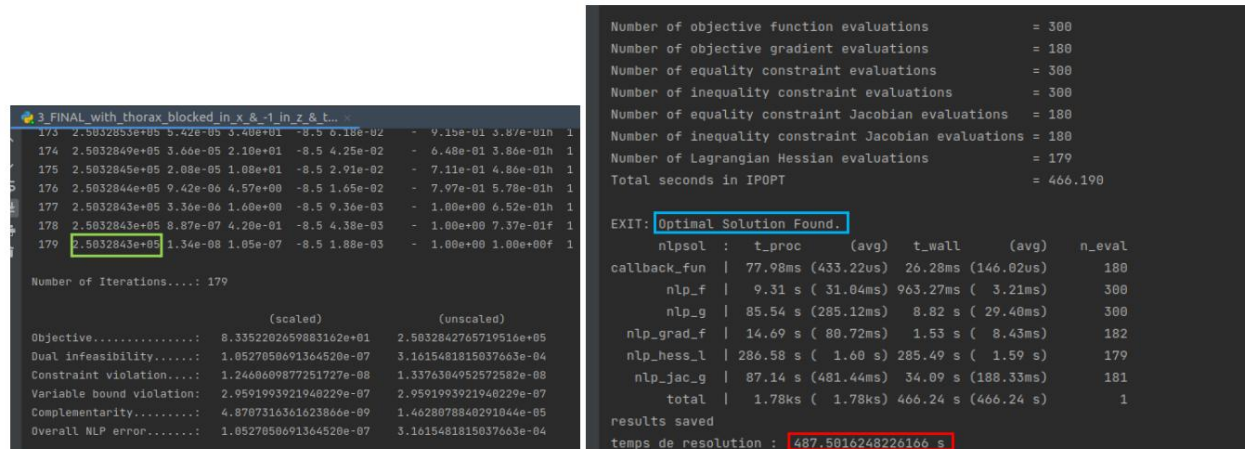
## Caption :

EXIT: Optimal Solution Found. The program found an optimal solution, that is, a solution that converged.

temps de resolution : 193.3928849697113 s : The code took 193.3928849697113 seconds to find a solution.

7.0017991e+03 : The sum of the program objectives (size of an objective = weight\*values) is 7.0017991e+03.

# Appendix G: Optimal Solution found 2



**Figure Annex - 8:** Optimal solution found by the program for a pressed staccato playing with particular minimization.

## Caption :

EXIT: Optimal Solution Found. The program found an optimal solution, that is, a solution that converged.

temps de resolution : 487.5016248226166 s : The code took 487.5016248226166 seconds to find a solution.

2.5032843e+05 : The sum of the program objectives (size of an objective = weight\*values) is 2.5032843e+05.

## Appendix H: Optimal Solution found 3

```

afficher_animation_bioviz x 100 x afficher_bioMod_bioviz x
66 1.8788887e+04 3.00e-08 6.17e-05 -5.7 2.47e-03 - 1.88e+08 1.88e+08 1
67 1.8779979e+04 5.56e-05 7.44e+00 -7.1 9.81e-02 - 7.40e-01 7.04e-01 1
68 1.8779972e+04 2.91e-05 1.89e+01 -7.1 6.76e-02 - 1.00e+00 6.39e-01 1
69 1.8779968e+04 1.05e-05 2.52e+00 -7.1 4.30e-02 - 1.00e+00 8.67e-01 1
iter objective inf_pr inf_du lg(mu) ||d|| lg(rg) alpha_du alpha_pr ls
70 1.8779968e+04 8.30e-07 2.16e-06 -7.1 1.04e-02 - 1.00e+00 1.00e+00 1
71 1.8779968e+04 2.59e-09 1.07e-08 -7.1 5.40e-04 - 1.00e+00 1.00e+00 1

Number of Iterations....: 71

(scaled) (unscaled)
Objective.....: 1.5552981309903862e+02 1.8779968011840785e+04
Dual infeasibility.....: 1.0669108593607905e-08 1.2882772383660104e-06
Constraint violation....: 1.5843593104136744e-10 2.5943162063057912e-09
Variable bound violation: 4.8071454039622897e-09 4.8071454039622897e-09
Complementarity.....: 8.0903115280567038e-08 9.7689175261839349e-06
Overall NLP error.....: 8.0903115280567038e-08 9.7689175261839349e-06

```

```

Number of objective function evaluations = 84
Number of objective gradient evaluations = 72
Number of equality constraint evaluations = 84
Number of inequality constraint evaluations = 84
Number of equality constraint Jacobian evaluations = 72
Number of inequality constraint Jacobian evaluations = 72
Number of Lagrangian Hessian evaluations = 71
Total seconds in IPOPT = 163.360

EXIT: Optimal Solution Found.

nlp_sol : t_proc (avg) t_wall (avg) n_eval
callback_fun | 91.06ms ( 1.26ms) 16.17ms (224.57us) 72
nlp_f | 2.56 s ( 30.42ms) 257.65ms ( 3.07ms) 84
nlp_g | 26.53 s (315.89ms) 2.66 s ( 31.69ms) 84
nlp_grad_f | 5.46 s ( 73.76ms) 553.02ms ( 7.47ms) 74
nlp_hess_l | 110.20 s ( 1.55 s) 109.41 s ( 1.54 s) 71
nlp_jac_g | 35.96 s (492.67ms) 13.35 s (182.92ms) 73
total | 503.38 s (503.38 s) 163.36 s (163.36 s) 1

results saved
temps de resolution : 183.98191285133362 s

```

**Figure Annex - 9:** Optimal solution found by the program for a staccato hit game without any particular minimization.

### Caption :

- The program found an optimal solution, that is, a solution that converged.
- : The code took 183.981913285122262 seconds to find a solution.
- : The sum of the program objectives (size of an objective = weight\*values) is 1.8779968e+04.

## Annex I: Optimal Solution found 4

```

afficher_animation_bioviz x 2_with_thorax_blocked_in_x & -1_in_z & thorax ... x
207 8.1475019e+05 1.61e-05 2.93e+01 -8.6 1.30e-01 - 8.79e-01 2.60e-01 1
208 8.1475002e+05 5.69e-04 1.02e+01 -8.6 9.95e-02 - 8.97e-01 6.66e-01 1
209 8.1474995e+05 1.70e-04 3.00e+00 -8.6 3.62e-02 - 1.00e+00 7.12e-01 1
iter objective inf_pr inf_du lg(mu) ||d|| lg(rg) alpha_du alpha_pr ls
210 8.1474994e+05 8.06e-05 1.42e+00 -8.6 1.08e-02 - 1.00e+00 5.26e-01 1
211 8.1474993e+05 5.26e-06 8.91e-02 -8.6 5.04e-03 - 8.13e-01 9.37e-01 1
212 8.1474993e+05 1.77e-09 7.43e-09 -8.6 4.78e-04 - 1.00e+00 1.00e+00 1

Number of Iterations....: 212

(scaled) (unscaled)
Objective.....: 1.3495087430201395e+02 8.1474992738964909e+05
Dual infeasibility.....: 7.4277019636201695e-09 4.4844137113907271e-05
Constraint violation....: 1.7577849939498513e-09 1.7744458680191144e-09
Variable bound violation: 2.9604645135350438e-07 2.9604645135350438e-07
Complementarity.....: 2.9075912118779168e-09 1.7554341789057921e-05
Overall NLP error.....: 7.4277019636201695e-09 4.4844137113907271e-05

```

```

Number of Iterations....: 212

(scaled) (unscaled)
Objective.....: 1.3495087430201395e+02 8.1474992738964909e+05
Dual infeasibility.....: 7.4277019636201695e-09 4.4844137113907271e-05
Constraint violation....: 1.7577849939498513e-09 1.7744458680191144e-09
Variable bound violation: 2.9604645135350438e-07 2.9604645135350438e-07
Complementarity.....: 2.9075912118779168e-09 1.7554341789057921e-05
Overall NLP error.....: 7.4277019636201695e-09 4.4844137113907271e-05

Number of objective function evaluations = 320
Number of objective gradient evaluations = 213
Number of equality constraint evaluations = 320
Number of inequality constraint evaluations = 320
Number of equality constraint Jacobian evaluations = 213
Number of inequality constraint Jacobian evaluations = 213
Number of Lagrangian Hessian evaluations = 212
Total seconds in IPOPT = 486.821

EXIT: Optimal Solution Found.

nlp_sol : t_proc (avg) t_wall (avg) n_eval
callback_fun | 31.58ms (148.27us) 23.77ms (111.59us) 213
nlp_f | 9.36 s ( 29.24ms) 874.80ms ( 2.73ms) 320
nlp_g | 94.47 s (295.21ms) 8.72 s ( 27.25ms) 320
nlp_grad_f | 16.69 s ( 77.64ms) 1.56 s ( 7.28ms) 215
nlp_hess_l | 319.38 s ( 1.51 s) 318.20 s ( 1.50 s) 212
nlp_jac_g | 118.17 s (552.21ms) 38.38 s (178.96ms) 214
total | 1.70ks ( 1.70ks) 486.82 s (486.82 s) 1

results saved
temps de resolution : 505.8667092323303 s

```

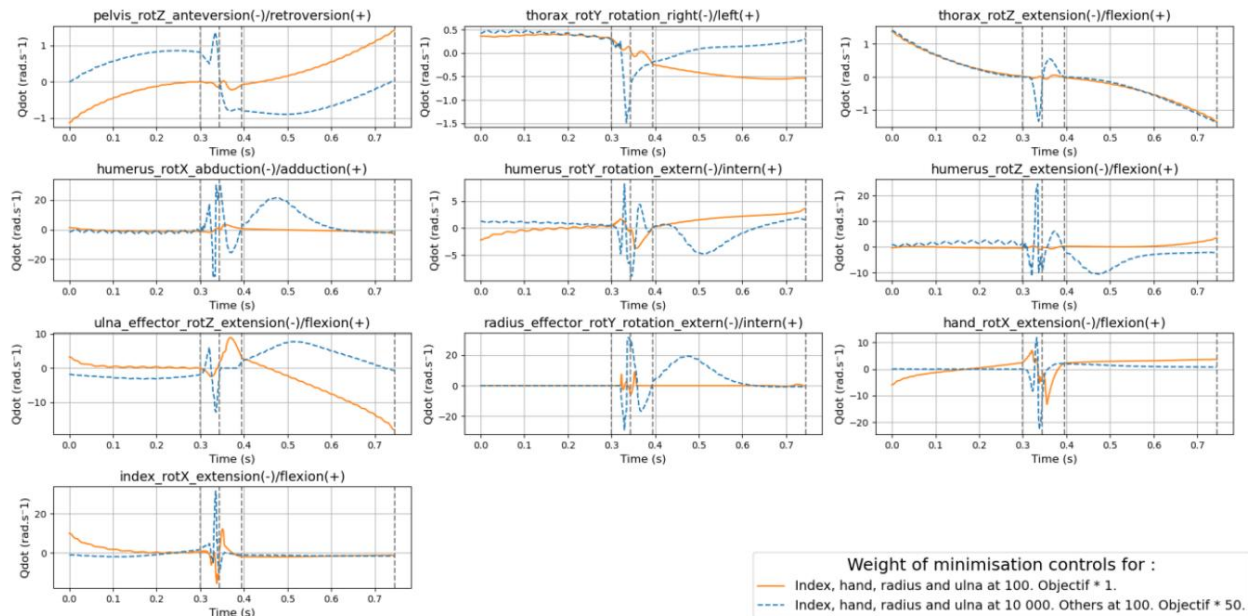
**Figure Appendix - 10:** Optimal solution found by the program for a staccato hit game with particular minimization.

### Caption :

- The program found an optimal solution, that is, a solution that converged.
- : The code took 505.8667092323303 seconds to find a solution.
- : The sum of the program objectives (size of an objective = weight\*values) is 8.147e+05.

## Appendix J: Angular Velocities - Squeezed Set

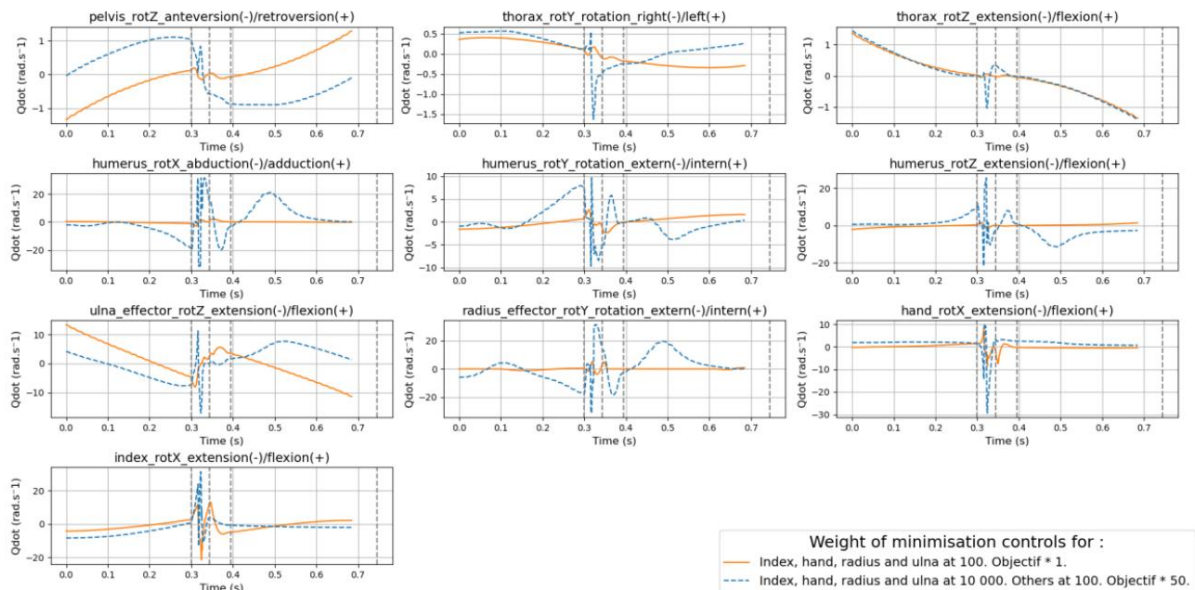
States ( $\dot{q}$ ) of limbs by minimizing more the finger, hand, radius & ulna for a staccato pressed attack of one key.



**Figure Appendix - 11 :** Joint velocities (in rad/s) of the 10 degrees of freedom of the model as a function of time (s) for a staccato pressed game for two different simulations.

## Appendix K: Angular Velocities - Slap Game

States ( $\dot{q}$ ) of limbs by minimizing more the finger, hand, radius & ulna for a staccato struck attack of one key.



**Figure Appendix - 12:** Joint speeds (in rad/s) of the 10 degrees of freedom of the model as a function of time (s) for a staccato hit game for two different simulations